

AE-141

UDC 536.24  
621.039.534

AE-141

# Heat Transfer and Pressure Drop with Rough Surfaces, a Literature Survey

A. Bhattacharyya



AKTIEBOLAGET ATOMENERGI  
STOCKHOLM, SWEDEN 1964



HEAT TRANSFER AND PRESSURE DROP WITH ROUGH SURFACES,A LITERATURE SURVEY

Ajay Bhattacharyya

Summary:

This literature survey deals with changes in heat transfer coefficient and friction factor with varying nature and degree of roughness. Experimental data cover mainly the turbulent flow region for both air and water as flow mediums. Semiempirical analysis about changes in heat transfer coefficient due to roughness has been included. An example of how to use these data to design a heat exchanger surface is also cited. The extreme case of large fins has not been considered. Available literature between 1933 - 1963 has been covered.

## LIST OF CONTENTS

	Page
Summary	1
1. Introduction	3
2. Classification	4
2.1. Roughness elements	4
2.2. Flow	6
3. Effect of roughness elements on friction factor	7
3.1. Laminar region	7
3.2. Turbulent region subdivisions	7
4. Effect of roughness elements on heat transfer	8
4.1. Laminar region	8
4.2. Turbulent region	9
5. Effect of roughness elements on boundary layer transition	11
6. Semi-empirical relations for sand-type roughness	12
7. Heat transfer and friction factor - experimental data for AIR	16
7.1. Circular tube with square thread type roughness	16
7.2. Circular tube with wire-coil type roughness	20
7.3. Circular tube with circumferential rings	21
7.4. Rectangular duct of small hydraulic diameter with integral roughness elements	24
7.5. Rectangular channel with bottom half roughened	25
7.6. Annular channel with inner tube roughened	28
8. * Heat transfer and friction factor - experimental data for WATER	32
8.1. Circular tube with sand-grain type roughness and commercial pipes (air)	32
8.2. Annular channel with inner tube roughened	34
9. Friction factor	41
9.1. Circular tube with drilled holes as roughness elements	41
9.2. Annular channel with inner tube roughened	41
10. Transformation of experimental data	42
11. Practical application	44
Acknowledgement	45
List of notations	46
References	50
Figures	55

## Introduction

Lately the idea of improving heat transfer performance of a surface by introducing artificial roughness elements has gained some ground. Effect of various kinds of roughness elements on friction factor has been studied both experimentally and theoretically with the help of semi-empirical equations. It is only recently the question of the effect of various roughness elements on coefficient of heat transfer has been taken up in greater detail. Most of the data available today is for forced convection turbulent flow systems. In the ideal case one wants to predict the friction factor and coefficient of heat transfer once the geometry of the surface is known. However, the number of parameters necessary to describe the geometry of a surface is so many that it is hardly likely that a completely general relation in terms of geometrical and flow parameters, not too difficult to handle, will be found.

Improvement in the heat transfer process is accompanied by correspondingly larger increase in the skin-friction. However, in some cases, it is desirable to provide a rough surface to increase the heat transfer rate where space is more important to power loss as a result of increased pressure drop. Economic advantage of using roughened surface, in all probability, will not arise from increased thermal performance but from a reduction in the quantity of material used or from simplification in design due to possibilities of using lower velocities. As an example, the case of a nuclear reactor where stainless steel is used as the casing material can be cited. One way of improving heat transfer performance is using fins. Stainless steel, however, has a very poor thermal conductivity. As a result of which the efficiency of stainless steel fins is very low. There is also a need to minimize the quantity of stainless steel used in a nuclear reactor owing to its high neutron absorption. On the other hand, without fins the surface area required to transmit a particular amount of heat is too large. A balance can be achieved by roughening the

heat transfer surface artificially at the expense of higher pressure loss.

## 2. Classification

### 2.1. Roughness elements

Before discussing the different approaches utilized in presenting the experimental data in the following literature survey, an attempt will be made to classify roughness elements from both physical and fluid mechanics points of view.

Physically artificial roughness can be of two types:

- a. integral
- b. superimposed

Integral roughness elements are integral part of the main surface. They can be either two or three dimensional. Randomly distributed sand-grain type roughness can be designated as three-dimensional. Roughness in the commercial pipes is also three dimensional. Protrusions in the form of rivet-heads or depressions in the form of drilled holes can also be termed as three dimensional.

The following types of roughness elements are loosely termed as two dimensional.

1. Grooves parallel or perpendicular to the direction of flow of the heat exchanger medium.
2. Ribs parallel or perpendicular to the direction of flow of the heat exchanger medium. (Ribs may or may not be chamfered.)
3. Threads perpendicular to the direction of flow of the heat exchanger medium.

Superimposed roughness elements are usually two dimensional. Superimposed roughness elements can be termed pure turbulence promoters. The contact thermal resistance between the superimposed roughness elements and the main surface is so high that unlike the integral type roughness elements they do not contribute anything towards increasing the area of heat transfer. However, it should be mentioned that normally the increase in heat transfer area with integral type is also very little. Superimposed roughness elements are usually of the form of wire-coil wound on the surface. Different wire cross-sections like circular or square can be used. Nunner (28), even, tested roughness elements of the form of piston rings fitted inside circular tubes.

Friction Factor:

The friction factor "f" is defined by the following equation:

$$\frac{dP}{dL} = \frac{f}{D} \cdot \frac{1}{2} \cdot \rho \cdot w^2 \quad (1)$$

"f" is a dimensionless factor. A functional relationship of the following form can be written also. (26)<sup>1</sup>.

$$f = F(\text{Re}, k/D, p/D, s/D, \dots) \quad (2)$$

More dimensionless geometrical parameters can be incorporated in the relation above, if it is found necessary, to describe the roughness elements more fully.

Longitudinal spacing of the roughness elements i. e. "p" is one of the more important parameters. Each roughness element disturbs the main flow in the way that it gives rise to vorticity which is swept downstream by the main flow. The longitudinal

---

1. Number inside bracket indicate reference number in the list of references.

frequency with which such sources of vorticity occur regulates the structure of turbulence also the energy dissipation phenomena.

## 2.2. Flow

Depending upon the distribution of roughness elements the flow can be divided into three basic types: (26)

- a. Isolated-roughness flow
- b. Wake-interference flow
- c. Quasi-smooth or skimming flow.

In the first case, behind a roughness element a vortex generating wake-zone is developed. However, the distance between the two consecutive elements is enough to allow the disturbances to die down. The friction factor is affected by the two following drags:

1. form drag on the roughness elements: controlling dimension for which, is height of the elements "k".
2. friction drag on the wall surface between elements which depends upon the distance between the two elements "p". So the parameter  $p/k$  can be expected to play an important role in this case.

In the case of wake-interference flow, as the name suggests, the wake zone behind one element overlaps with the wake zone of the next element. This happens when the elements are placed sufficiently close to each other. Major contribution to the friction factor comes from the intense turbulence in the space in between the elements. Thickness of the turbulent zone depends upon diameter of the pipe. So it appears that  $D/p$  will be an important parameter in this case.

The third type of flow which is termed as skimming flow occurs when the roughness elements are placed so close to each other that the flow essentially skips over the crests of the elements.

The flow regime can be divided into two parts:

- a. main turbulent flow in the center
- b. standing vortices in the grooves which are fed with energy from the main flow.

The combination of the roughness crests and the still water in the interstices serves as a psuedo-wall. This wall is a bit wavy in nature but it is without large roughness projections. The groove eddies are rectilinear circular vortices, having diameter equal to width of groove "b" or height of groove "k" (whichever is smaller). The number of such vortices depends on "p". The parameter  $p/k$  or  $p/b$  can, thus, be expected to be important in this type of flow.

### 3. Effect of roughness elements on friction factor

#### 3.1. Laminar region

In the laminar region resistance is practically the same for both smooth and rough pipes.

#### 3.2. Turbulent region subdivisions

Schlichting (34) has proposed the following subdivisions for the turbulent region:

a.  $0 < \frac{h v_*}{\nu} < 5$

In this region pipes of a given roughness behave in the same way as a smooth pipe. The size of the roughness elements is so small that all protrusions are contained within the laminar sub-

-layer (1). In this region the friction factor "f" is primarily a function of Reynolds number only. Goldstein (15) succeeded in deducing the limit of  $h v_* / \nu = 5$ : for the hydraulically smooth regime from the criterion that at that point a von Karman vortex street is about to begin to form on an individual protrusion.

$$b. \quad 5 < \frac{h v_*}{\nu} < 70$$

Here the height of the roughness elements exceed the laminar sub-layer. There is an increase in resistance due to two factors. Firstly it is due to form drag caused by the roughness itself and secondly due to the fact that the presence of roughness elements changes the velocity profile in its neighbourhood and the shearing stress on the wall. This is called the transition regime. The friction factor "f" is a function of both Reynolds number and a dimensionless roughness factor of the form  $h/r$ .

$$c. \quad \frac{h v_*}{\nu} > 70$$

In this region the height of the roughness elements definitely exceeds the thickness of the laminar sub-layer. The friction factor "f" becomes independent of Reynolds number. In this region which is termed "completely rough" the friction factor is only a function of a dimensionless factor of the form  $h/r$ .

The above analysis is valid for roughness obtained with sand. But for approximations these values have been utilized for experiments with other kind of roughness (12) (30).

#### 4. Effect of roughness elements on heat transfer

##### 4.1. Laminar region

In the laminar region roughness elements have no appreciable effect on heat transfer.

#### 4.2. Turbulent region

Nunner (28) has proposed a model to explain the mode of heat transfer in turbulent flow. In the case when the flow is fully developed it is assumed that the total frictional resistance can be divided into two parts.

- a. frictional resistance in the wall
- b. form resistance due to roughness elements.

It is further assumed that the roughness elements do not affect the viscous wall layer, i. e., it is assumed that the value of the wall shear stress is same as with a smooth tube. The roughness elements contribute to increased heat transfer by increasing the level of turbulence in the turbulent core. The form resistance gives rise to additional shear stress at a distance equal to the thickness of the viscous wall layer from the wall. The thickness of the viscous wall layer is assumed to be same in both rough and smooth tube. Beyond the viscous wall layer another layer called "roughness zone" is defined (see fig. 1 & 2). It is assumed that the value of the shear stress drops across the roughness zone and then it rises again across the viscous wall layer to the value same as in the smooth tubes. It is doubtful as to whether the assumption of the equal thickness of viscous layer in rough and smooth tubes is true. This model is quite different from the one proposed by Owen and Thomson (30), which is described below.

To explain the effect of roughness elements on heat transfer in the turbulent region Owen and Thomson (30) have proposed an interesting model for 3-dimensional roughness. Their model is applicable in the region "completely rough" and to make sure that no viscous sub-layer exists they propose that it is valid for  $h v_* / \nu > 100$ .

It is suggested that the presence of the protrusions gives rise to eddies "which wrap themselves around the individual excrescences"

ces and trail downstream (see fig. 3). The effect of these eddies is to draw fluid down into the valley-like regions between adjacent roughness elements which the fluid then scours before returning to mix with the main flow near the height of the roughness crests. It is suggested that the scouring action forms the basic convective mechanism of heat transfer at the wall. The heat is communicated to the fluid in the space near and beyond the roughness crests, which may be part of a turbulent boundary layer or pipe or channel, by the convective motion of the horseshoe-eddies. Major part of the heat transfer takes place in the sub-layer. Even though the crests of the roughness are subjected to faster moving flow the heat transfer area they present is small compared with the surface area swept by the sub-layer".

Edwards and Sheriff (12) from their tests with a single wire stretched across the flow path over a heat transfer surface came to following conclusions:

- a. To produce a significant effect on heat transfer:

$$k > 2 \cdot \delta_L$$

where

$$\delta_L = \text{thickness of laminar sub-layer} = \frac{5 \nu}{v_*}$$

$\delta_L = \delta_B =$  combined thickness of laminar sub-layer and buffer layer (12)

$k =$  height of the roughness element.

- b. For full effectiveness

$$k > \delta_B$$

- c. For  $\delta_B < k < 8 \cdot \delta_B$  there is no substantial change.

It is interesting to compare this result with the result obtained by Tani, Hama, and Mituisi (37) in their experiment on the permissible roughness in the laminar boundary layer. This critical value of the roughness is given by

$$h = \frac{15\nu}{v_*} = 3 \cdot \delta_L$$

It appears that the roughness elements become fully effective when the boundary layer transition has definitely taken place.

In their "five wire tests" Edwards and Sheriff (12) found that there is an unsteady vortex system behind the wire after which the main flow returns to the surface. The maximum improvement in heat transfer occurs in the region where the flow returns to the surface. Thermal entry length was reduced by the rough surface which indicated improved mixing of the fluid across the stream.

##### 5. Effect of roughness elements on boundary layer transition

This is important as far as thermal and hydrodynamic entry lengths are concerned. Apart from that one can get some idea about the shape of the flow when roughness elements are present. Liepmann and Fila (21 a) found that at low speeds the flow after passing over the roughness elements returned to the base surface still laminar and it remained laminar for some distance downstream. With higher speeds the transition to turbulent boundary layer took place immediately after the layer returned to the surface. With still higher speeds the flow became turbulent in the free boundary layer in the wake of the obstacle and returned to the surface in the turbulent state (see fig. 4).

## 6. Semi-empirical relations for sand-type roughness

Heat transfer and pressure drop phenomena in a smooth tube has been fairly extensively investigated. Semi-empirical or empirical relations are available for calculating these coefficients. Some general relations regarding friction factor will be presented here to facilitate comparison with the relations presented later on with respect to rough surfaces (28) (34).

Smooth tubes: In the laminar flow region "f" is a function of Reynolds number and it is given by the following relation:

$$f = \frac{64}{Re} \quad (3)$$

The following empirical relation is due to Blasius and it is valid in the region  $Re < 100000$

$$f = \frac{0.3164}{Re^{0.25}} \quad (4)$$

For higher Reynolds numbers Prandtl's universal law of friction for smooth pipes can be used.

$$\frac{1}{\sqrt{f}} = 2.0 \log (Re \sqrt{f}) - 0.8 \quad (5)$$

It has been verified by J. Nikuradse's experiments upto a Reynolds number of  $3.4 \times 10^6$  and the agreement is seen to be excellent.

In the completely rough region (34) resistance formula for sand roughened pipes is:

$$f = \frac{1}{\left(2 \log \frac{R}{h} + 1.74\right)^2} \quad (6)$$

where "h" denotes the grain size in Nikuradse's sand roughness. Colebrook and White (19) established an equation which correlates the whole transition region from hydraulically smooth to completely rough flow:

$$\frac{1}{\sqrt{f}} = 1.74 - 2 \log \left( \frac{h}{R} + \frac{18.7}{\text{Re} \sqrt{f}} \right) \quad (7)$$

Schlichting (34) has given a method for correlating friction data for roughness elements which cannot be described as sand roughness. Schlichting's method is based on finding for any given roughness the equivalent sand roughness. The equivalent sand roughness is that value of roughness which when inserted into equation 7 gives the actual resistance. The table reproduced from the reference 34 gives the value for some regular roughness patterns (see fig. 5). For a fully turbulent, steady, hydrodynamically and thermally established flow in a rough pipe Dipprey (8) presents generalised relations for heat transfer and friction factor. Regarding the roughness it is assumed that the surface roughness patterns are statistically independent of circumferential or axial position and they are statistically geometrically similar from tube to tube with only a geometrical scale factor being different. From semi-empirically considerations the following friction similarity law is given

$$\left[ \frac{8}{f} \right]^{1/2} = -B \ln \frac{2k}{D} + A [K^*] - E \quad (8)$$

where,  $K^* = \frac{k v_*}{\nu} = \text{Re} \cdot \left[ \frac{f}{8} \right]^{1/2} \cdot \frac{k}{D}$

The function  $A [K^*]$  is a general function determined empirically for each roughness shape, and  $B = 2.50$ ,  $E = 3.75$ .

The fig. 6 shows  $A [K^*]$  vs.  $K^*$  for Nikuradse's sand-grain roughness. The heat transfer similarity law is given as:

$$\frac{\frac{f}{8St} - 1}{\left[\frac{f}{8}\right]^{1/2}} + A = g\left[K^*, Pr\right] \quad (9)$$

where,  $A = \text{constant value of } A\left[K^*\right]$  for the fully rough region. Using  $A = 8.48$ ,  $g\left[K^*, Pr\right]$  for the tubes tested by Dipprey is shown in the fig. 7 & 8.

It is observed that in the fully rough region ( $K^* > 67$ ) the curves become parallel on the log-log plott which is reproduced from ref. 8. For  $g\left[K^*, Pr\right]$  in the fully developed region Dipprey arrives at the following expression:

$$g_{FR} = K_f \cdot K^{*m} \cdot Pr^n \quad (10)$$

for the roughness investigated by Dipprey:

$$K_f = 5.19, \quad m = 0.20 \quad \text{and} \quad n = 0.44$$

Fig. 9 indicates that Dipprey's theory predicts the values  $\frac{8St}{f}$  in quite a reasonable fashion over a wide range of Prandtl's numbers.

Owen and Thomson (30) independently have proposed a similar correlation as Dipprey's. A sub-layer Stanton number is defined as follows:

$$q = \rho C_p v_* (T_h - T_s) St_{sub}$$

where sub-layer Stanton's number is given by the following relation:

$$St_{sub} = \frac{1}{E} \left[ \frac{v_* h}{v} \right]^{-m} \cdot [Pr]^{-n} \quad (11)$$

where  $m = 0.45$ ,  $n = 0.80$  and  $E = 0.45$  to  $0.7$  (see fig. 10). Fig. 10 indicates that the sublayer Stanton number is strongly dependent on Prandtl's number. The above relations are basically true for three dimensional roughness elements but they give good correlations for some two dimensional roughness also. As an example circumferential rings tested by Nunner (28) can be mentioned.

Apart from the correlations proposed by Owen and Thomson and by Dipprey there are two more equations which have been frequently tested for their validity.

The older one of the two is Martinelli's equation. It is as follows:

$$St. Pr_f^{2/3} = \frac{\sqrt{\frac{f}{8}} Pr^{2/3} \Delta t_{max} / \Delta t_{mean}}{5 [Pr + 1.4 \ln(1 + 5Pr) + 0.5 D.R. \ln Re / 60 \sqrt{f/8}]} \quad (12)$$

Smith and Epstein (37) and Kemeny and Cyphers (20) found that the above equation agrees fairly well with some of their data. At the "completely rough" region where "f" becomes independent of Re the factor  $St. Pr_f^{2/3}$  keeps still decreasing with this equation. This agrees qualitatively very well with data of Sams (33), Epstein (37), Cope (5) and Walker (39).

The other equation was proposed by Nunner (28). It has the shortcoming that it fails to predict the behaviour which Martinelli's and Dipprey's equation do so successfully. Moreover, for

medium other than air Nunner's equation gives a rather poor correlation. The equation is as follows:

$$\text{Nu} = \frac{f/8 \text{ Re Pr}}{1 + 1.5 \text{ Re}^{-1/8} \text{ Pr}^{-1/6} (\text{Pr} f/f_0 - 1)} \quad (13)$$

## 7. Heat transfer and friction factor - experimental data for AIR

### 7.1. Circular tube with square thread type roughness

Sams (33) studied the effect of square-thread type roughness on the heat transfer process in a circular tube. Data were obtained for air flowing through a tube of 12.7 mm diameter. Maximum Reynolds number was  $3.5 \times 10^5$  and the maximum average inside-surface temperature was  $805^\circ\text{C}$ . Three different kinds of threads were investigated:

Type	$\frac{\text{height of the thread}}{\text{radius of the tube}} = \frac{k}{r}$
A	0.025
B	0.037
C	0.016

Evaluating all the physical properties at the wall temperature the following correlations were obtained by Sams (33). Air velocity in all cases was evaluated at the average bulk temperature of the fluid.

For the smooth tube:

$$\text{Nu} = 0.023 \text{ Re}^{0.8} \cdot \text{Pr}^{0.4} \quad (14)$$

For the rough tube the characteristics length used is the mean diameter between the root and the tip of the threads.

for the rough tube "A":

$$Nu = 0.0070 Re^{0.95} \cdot Pr^{0.4} \quad (15)$$

for the rough tube "B":

$$Nu = 0.0087 Re^{0.92} \cdot Pr^{0.4} \quad (16)$$

for the rough tube "C":

$$Nu = 0.016 Re^{0.84} \cdot Pr^{0.4} \quad (17)$$

In the conventional form of Reynolds number the velocity used is the mean velocity of the fluid in the tube. This means that velocity is almost independent of the degree or nature of roughness. On the other hand, friction coefficient is directly related to the nature of the roughness elements. To incorporate the friction factor in the dimensionless correlation Sams proposes a modified Reynolds number. Instead of the mean velocity, friction velocity  $v_*$  is used in the Reynolds number.

Using film temperature to evaluate the physical properties, for square-threaded type of roughness in circular tubes the following correlation was obtained by Sams.

$$Nu = 0.040 Re_{mod}^{1.0} \cdot Pr^{0.4}$$

$$\text{where, } Re_{mod} = \frac{\rho_f v_* \cdot D}{\mu_f} \quad \text{and } v_* = w \cdot \sqrt{\frac{f}{8}} \quad (18)$$

The maximum scatter of the data is less than 15 % with this correlation. By comparing fig. 11 and fig. 12 one notices how the experimental points crowd towards a single line with the use of friction velocity in the modified Reynolds number.

Following empirical dimensionless correlations were proposed for calculating friction factor for the tubes investigated from the geometrical parameters.

For  $0.88 < \frac{k}{b} < 1.37$ ,  $1.0 < \frac{p}{b} < 7.06$  and  $0.011 < \frac{k}{r} < 0.039$ :

$$\frac{f}{8} = 0.0036 \left(\frac{p}{b}\right)^{0.8} \left(\frac{k}{b}\right)^{1.70} \quad (19)$$

Sams's data indicates that at lower Reynolds number the roughness elements affect the heat transfer process less than what it does at higher Reynolds numbers. The explanation put forward to account for this phenomena is that at higher Reynolds numbers the thickness of the boundary layer decreases to a point that the roughness elements protrude beyond the viscous sub-layer. Nunner's (28) experimental results are exactly opposite to this, i. e. in Nunner's experiment the effect of roughness on heat transfer decreased with increasing Reynolds number. Fig. 13 indicates how the friction factor "f" for different tubes tested varies with Reynolds numbers.

Following von Kármán's analysis (19) and utilizing Sams's experimental data (33) Pinkel (31) arrived at some semi-empirical dimensionless relations giving friction factor and coefficients of heat transfer for the rough tubes investigated. Nusselts number evaluated at the film temperature turns out to be a function of the following form:

$$Nu = F(Re, Pr, \frac{h}{D}, f)$$

where,  $f = F(Re, \frac{h}{D})$ .

$\frac{h}{D}$  is the conventional roughness ratio where "h" denotes the effective thickness of layer associated with roughness. The dimensionless relations are as follows:

$$A \cdot \frac{Nu}{Pr^{0.4}} = 0.023 Re^{0.8} \quad (20)$$

$$\text{where, } A = \frac{8}{0.023f} \cdot \left[ 0.91 + 1370 \frac{h}{26D} \sqrt{\frac{f}{8}} \right] \cdot \frac{Re^{-0.2}}{Pr^{0.6}}$$

$$\text{and } \sqrt{\frac{8}{f}} = \sqrt{8} \left[ 2 \log \frac{\frac{1}{2} \cdot Re \cdot \sqrt{\frac{f}{8}}}{1 + \frac{h}{26D} \cdot Re \cdot \sqrt{\frac{f}{8}}} + 0.705 \right]$$

In the above equations the physical properties are evaluated at the film temperature. The film temperature is calculated in the following way:

$$T_f = \frac{T_b + T_s}{2}$$

Only while calculating the velocity the bulk temperature of the fluid is used.

In the fig. 14 a  $\frac{A \cdot Nu}{Pr^{0.4}}$  is plotted against Re for the tubes of various roughness and for a range of  $\frac{T_s}{T_b}$  from 1.4 to 2.5. In the fig. 14 b is shown a plott of "A" against Re with  $\frac{h}{26D}$  as a parameter. Fig. 14 a indicates that the equation 20 is in good agreement with the experimental data.

The roughness factor  $\frac{h}{26D}$  is a function of the several dimensions of the roughness elements. Because of this fact the practical utility of the above relations is limited. However, they indicate how friction factor affects the heat transfer rate in square-threaded type roughness.

7.2. Circular tube with wire-coil type roughness

Sams (32) also studied heat transfer and pressure drop characteristics in circular tubes with roughness elements consisting of wire-coil. This type of roughness elements contribute mainly towards promoting turbulence and not so much to the increase in the overall heat transfer surface. The contact resistance between the wire-coil and the inner surface of the tube is very high compared to the resistance of the tube wall. As a result, the contribution of the wire-coil to the increase in the heat transfer surface is negligible. In the test the highest value of the Reynolds number was  $10^5$  and the maximum wall temperature was  $568^\circ\text{C}$ .

In all calculations the inner diameter of the smooth tube is used as the characteristics length. The only exception is in the case where  $p/k = 1$ . Then the inner diameter of the coil is used as the characteristics length.

The following table gives an idea about the different coils tested. The table is computed from a similar table given in the ref. 32.

Table Inside diameter of the tube = 10.4 mm

Wire diameter = k	Coil-pitch = p	p/k	$t_{s_{\max}}$	$T_s/T_{b_{\max}}$
mm	mm		$^\circ\text{C}$	
0.66	41.4	62.7	228	1.38
0.66	26.2	39.6	224	1.34
0.66	12.4	18.8	426	1.55
0.66	6.66	10.0	217	1.28
0.66	3.3	5.0	570	1.64
0.66	0.66	1.0	239	1.40
0.48	15.7	32.6	229	1.34
0.48	6.6	13.7	218	1.28
0.48	2.5	5.3	210	1.26
0.48	0.48	1.0	235	1.38
0.33	55.4	168.2	239	1.40
0.33	30.2	91.5	236	1.38
0.33	17.5	53.1	222	1.35
0.33	12.4	37.7	239	1.37
0.33	6.9	20.8	218	1.29

Sams (32) uses a modified Reynolds number to correlate his data. The modified Reynolds number is defined as follows:

$$Re_{\text{mod}} = \frac{\rho_s \cdot w_b \cdot D}{\mu_s}$$

where the subscript "s" denotes the properties evaluated at the average inner surface temperature of the tube and the subscript "b" denotes the quantities evaluated at the bulk temperature. The correlation in the conventional form is given below.

$$Nu_s = 0.023 Re_{\text{mod}}^{0.8} \cdot Pr_s^{0.4} \quad (21)$$

In the fig. 15  $\frac{Nu_s}{Pr_s^{0.4}}$  is plotted against  $Re_{\text{mod}}$  for different pitch to diameter ratio for the 0.66 mm coil. It indicates that with decreasing coil-pitch the rate of heat transfer increases. At a certain pitch to diameter ratio a maxima occurs and after that the heat transfer ratio starts decreasing. The maximum value of  $\alpha/\alpha_o$  is slightly different for different coils and the pitch to diameter ratio at which it occurs is also different. The maximum value of  $\alpha/\alpha_o$  lie between  $p/k = 7$  and  $p/k = 10$ . Fig. 16 gives an idea about the variation.

Similar to the heat transfer rate the friction factor increases with smaller pitch. The maximum friction factor relative to the smooth tube occurs when the coil pitch is equivalent to 7 or 8 wire diameters. Fig. 17 shows the variation of  $f/f_o$  with  $p/k$ . Fig. 18 shows the variation of heat transfer to friction ratio with  $p/k$ .

### 7.3. Circular tube with circumferential rings

Nunner (28) studied heat transfer and pressure drop in air flow through pipes roughened by circumferential rings. Different

arrangements with several widths and spacings of the rings were tested. Reynolds number was varied from 500 to  $8 \cdot 10^4$ .

By studying the experimental results Nunner arrived at the following relations:

$$\text{when } 1 < \frac{f}{f_o} < 6,$$

$$\frac{Nu}{Nu_o} = \left[ \frac{f}{f_o} \right]^{1/m} \quad (22)$$

$$\text{where, } m = \left[ \frac{Re}{100} \right]^{1/8}$$

In calculating the Nusselts number and Reynolds number the characteristics length is " $d_M$ " which is given by the following relation:

$$d_M = \sqrt{\frac{4V}{\pi L}} \quad (23)$$

where, "V" is the volume of the fluid filling the tube in question over a length "L".

For turbulent flow " $Nu_o$ " and " $f_o$ " can be substituted with the following wellknown relations:

$$Nu_o = 0.024 Re^{0.786} \cdot Pr^{0.45} \quad (24)$$

$$\text{and } f_o = (100 Re)^{-1/4} \quad (25)$$

For air ( $Pr = 0.72$ ) one arrives at the following relation which is valid for  $f < 0.13$ :

$$\text{Nu} = 0.383 \text{Re}^{0.68} \cdot f^{1/m} \quad (26)$$

for  $f/f_o \leq 3$  and  $\text{Re} \leq 10^5$ .

"m" can also be calculated from the following relations:

when  $\text{Pr} \geq 1$

$$m = \frac{\text{Pr}}{2} + 1.5 \quad (27)$$

when  $\text{Pr} < 1$

$$m = \text{Pr} + 1.1 \quad (28)$$

However, it should be pointed out that Nunner's results do not agree particularly well with other test results for fluids with Prandtl number greater than 1. Nunner also derived a general heat transfer equation for smooth and rough tubes. Though this semi-empirical equation does not agree uniformly with the experimental data yet it is quite useful in approximating effects of different dimensionless parameters. The equation is as follows:

$$\text{Nu} = \frac{\frac{f}{8} \cdot \text{Re} \cdot \text{Pr}}{1 + 1.5 \text{Re}^{-1/8} \cdot \text{Pr}^{-1/6} \cdot \left[ \text{Pr} \cdot \frac{f}{f_o} - 1 \right]} \quad (29)$$

The above equation is derived on the basis of following assumptions:

- a. at the root of the roughness elements the shear stress is same as it is with a smooth tube.
- b. the shearing stress decreases to some extent in the viscous sub-layer. It increases again in the roughness zone, corresponding to the additional shape resistance.

- c. the flow is assumed to be established. The shearing stress decreases linearly in the turbulent core to the value of zero in the centre. Fig. 1 and 2 illustrates the assumptions.

The above equation implies that the relation between friction factor and heat transfer coefficient is unique. Neither Dipprey's (8) experimental and theoretical results nor Walker's experimental results corroborate this.

#### 7.4. Rectangular duct of small hydraulic diameter with integral roughness elements

Lancet (21) studied the effect of surface roughness on heat transfer for fully developed turbulent flow in ducts with uniform heat flux. The duct had following dimensions:

maximum width = 3.68 mm

maximum height = 1.14 mm

The protrusions were approximately 0.25 mm x 0.25 mm x 0.25 mm and were spaced approximately 0.25 mm apart. The hydraulic diameter was of the order of 0.89 mm. and Reynolds number was varied from 3000 to  $2.77 \cdot 10^4$ .

Experimental data for the rough duct was correlated by the following dimensionless equation:

$$\text{Nu} = 0.042 \text{Re}^{0.8} \cdot \text{Pr}^{1/3} \quad (30)$$

Nunner's (28) theoretical equation agrees quite well with Lancet's data at higher Reynolds numbers (see fig. 19).

Another interesting result of the experiment is that in narrow ducts very fine scratches are sufficient to affect the heat transfer process. The surface finish in the smooth tube corresponds to a

radius to protrusion height ratio of the order of 150. Improvement of the coefficient of heat transfer was of the order of 15 %.

The results of the experiment are said to be valid for fully turbulent flow. This might not be quite correct because the total length of the test piece is about  $130 d_H$ . In the case of rough tube one needs about  $40 d_H$  to have a fully developed turbulent flow. So in all probability over a part of the length over which the mean coefficient of heat transfer are calculated the flow is not fully developed.

#### 7.5. Rectangular channel with bottom half roughened.

Fournel (13) suggested the following criterion to find when a roughness element of wire-wound type is most effective.

- a. The wire diameter "k" should be of the same order as the laminar boundary layer thickness.
- b. The pitch "p" should be of the same order as the length of the wake. If too small the downstream element lies in the wake of the roughness elements causing unnecessary drag. If the pitch is too large then the laminar boundary layer gets a chance to reform. That leads to increased thermal resistance.

Fournel's experimental data were obtained in a rectangular channel (1 cm x 8 cm) with air as the flow medium. Only the bottom half of the channel was roughened. Two wire patterns were tested. They were as follows:

- a. crossed wires  $k = 0.5 \text{ mm}$
- b. parallel wires  $k = 0.9 \text{ mm}$ .

Reynolds number range is approximately  $1.7 \cdot 10^4$  to  $5.8 \cdot 10^4$ . Experimental data indicates  $St/f$  ratio decreases from the smooth surface value when wire patterns are superimposed on it. The following table illustrates the statement.

Type of roughness	St/f
smooth	0.155
cross-wired	0.135
parallel-wired	0.120

Fournel's presentation of data is not very elaborate. The Stanton vs. Reynolds number plot indicates that the relation is almost linear and at higher Reynolds numbers the distance between the smooth surface curve and the wire wound surface curve increases for the cross wired surface. The distance decreases in the case of parallel-wired surface. It might be mentioned in this connection that Draycott and Lawther (10) found that their experimental data on wire-wound surface did not give a linear relationship.

Edwards and Sheriff (12) conducted an experiment in a rectangular wind-tunnel of 61.7 cm width and 5.1 cm height. Only the lower wall of the channel was roughened. This was also the only heated wall. Roughening was done by cementing circular sectioned wires to the surface at right angles to the direction of air flow. Heat flux was kept uniform over the surface. Reynolds number was varied from  $0.53 \cdot 10^5$  to  $0.86 \cdot 10^5$ .

In the single wire test, i. e., when only one wire was stretched across the flow path, they measured variation of local heat transfer coefficient on the smooth surface after the roughness element. The highest value of local heat transfer coefficient occurs at a distance which seems to be a function of Reynolds number. The following table computed from the graphs in the ref. 12 illustrates the point:

k = 1.59 mm

Re	distance/k
$0.53 \cdot 10^5$	10
$0.86 \cdot 10^5$	10
$1.23 \cdot 10^5$	6
$1.96 \cdot 10^5$	12

At  $Re = 1.23 \cdot 10^5$  the point where the maximum local heat transfer coefficient occurs the shifts towards the roughness element. Referring to the experiment on boundary layer transition done by Liepmann & Fila (21 a) it appears that probably round about this Reynolds number boundary layer transition takes place. Examining the curve showing the variation of local heat transfer coefficient for  $Re = 1.23 \cdot 10^5$  one notices that the values of the local heat transfer coefficient between 6k and 12k are rather irregular (see fig. 20).

In the test with multiple wires stretched across the flow path they found that in general higher values of  $\alpha/\alpha_0$  are obtained with smaller pitches between the wires. Naturally enough,  $f/f_0$  increases with smaller pitch.

Agreement with the values obtained by Nunner's expression with actual values obtained from the experiment is not particularly good. Unfortunately, in the absence of information about whether Hall's (17) modified Reynolds number or conventional Reynolds number was used in the calculations it is difficult to comment on the deviation. The table computed from ref. 12 is given below:

Pitch in centimeters	$\alpha/\alpha_0$ mean Nunner	$\alpha/\alpha_0$ mean Edwards & Sheriff
2.54		1.08
5.08		1.19
10.16		1.14
15.24		1.08
30.48		0.99

At the highest pitch the agreement is rather good but that is not of very much significance because at such high value of  $p/k = 192$  the effects of roughness is not so dominant.

The fig. 21 from ref. 12 indicates that when the height of the roughness elements is about 7 to 8 times the thickness of the laminar sublayer the value  $\alpha/\alpha_0$  nears a maxima. With increasing height of roughness there is slight increase in  $\alpha/\alpha_0$ . But friction loss increases at equal rate. Fig. 22 shows the variation of  $\alpha/\alpha_0$  between wires at various pitches.

#### 7.6. Annular channel with inner tube roughened

Draycott and Lawther (10) did a detail investigation of different kinds of roughened surfaces to find out their relative merits. The study included both integral types like threaded surfaces and superimposed types like wire-wound surfaces. The roughened surfaces were superimposed on a smooth cylindrical element of 49 mm outside diameter. The cylindrical element placed in a channel of 102 mm internal diameter formed an annular passage.

Heat transfer and pressure drop behaviour of the following surfaces were studied:

1. Smooth rod
2. Whitworth thread - 24, 18, 11, 5 threads per inch
3. Square grooved - 24, 18, 12, 6 grooves per inch
4. Wire-wound - wires of 0.91 mm and 1.62 mm diameter at pitches of 51 mm, 19 mm, 6.3 mm
5. Knurled - coarse and fine
6. Chamfered square ribs - half rib chamfered at  $10^\circ$ , 6 per inch  
full rib chamfered at  $10^\circ$ , 12 per inch.

Reynolds number range covered in the investigation was from  $0.5 \cdot 10^5$  to  $5 \cdot 10^5$ . The grooved surfaces gave improved values

of Stanton number without corresponding large increase in the friction factor. When the ribs across the flow path were chamfered Stanton numbers were still better. Unlike the grooved surfaces the wire-wound surfaces gave higher friction factors without adequate increase in the Stanton number. For the whitworth and knurled surfaces the experimental data could not be clearly correlated in terms of Stanton number and Reynolds number, according to Draycott and Lawther.

For the grooved surfaces and the smooth surface the heat transfer data were correlated with the help of an equation of the following form:

$$St = C \cdot Re^{-n} \tag{31}$$

where, "C" and "n" have following values:

Type of roughness	C	n
Smooth	0.029	0.21
Square grooved, 12 turns per inch	0.015	0.11
Square grooved, 6 turns per inch	0.018	0.09
Half rib width chamfered at $10^{\circ}$ , chamfer downstream		

For the grooved surfaces, logarithmic plot of friction factor vs. Reynolds number indicated that above  $Re = 1.5 \cdot 10^5$  there is a marked deviation from linearity. For the knurled surfaces this occurs at  $Re = 2 \cdot 10^5$ . Below this the friction factor for knurled surfaces is fairly constant. In the case of whitworth threaded surfaces the friction factor - Reynolds number relation is approximately linear.

Correction for Mach numbers:

At higher flow rates, the Mach numbers attained were of the order of 0.4 to 0.5. Since above  $M = 0.3$  compressibility effects

are not negligible a correlation of the following form is suggested by Draycott and Lawther (10).

$$St = F (Re, Pr, M) \quad (32)$$

Since,  $Pr = \text{constant}$  for this particular case of air as a medium, it can be rewritten as

$$St = F (Re, M) \quad (33)$$

For the wire-wound surfaces an exponential expression of the following form was obtained:

$$St = C \cdot Re^{-n} \cdot M^{-2n} \quad (34)$$

where "C" and "n" have following values:

Wire diameter = 0.91 mm gives  $n = 0.11$

Pitch in mm	C
6.3	0.017
19.0	0.014
51.0	0.011

Wire diameter = 1.62 mm gives  $n = 0.13$

Pitch in mm	C
6.3	0.020
19.0	0.019
51.0	0.015

From all the surfaces studied Draycott and Lawther found that the following surfaces give best improvement in heat transfer rates:

- a. Whitworth thread 24 threads per inch
- b. Square grooved, 12 threads per inch, full rib width chamfered at  $10^\circ$ , chamfer downstream.
- c. Square grooved, 6 threads per inch, half rib width chamfered at  $10^\circ$ , chamfer downstream.

Annular channel with the inner surface roughened with medium square grooved roughness:

Sheriff, Gumley and France (35) tested medium square grooved roughness of following dimensions using air as a flow medium in annuli with dimensions  $d_i = 25.4$  mm and  $d_o = 50.8$  and 76.2 mm.

k	p/k
0.25 mm & 0.51 mm	2.0
0.25 mm	5.0
0.25 mm	10.0

The Reynolds number range covered was  $10^4$  to  $10^5$ . The experimental data were correlated in the following way:

$$Nu = C \cdot Re^n \quad (35)$$

The following table indicates the different values of "n"

	p/k	$d_o = 50.8$ mm	$d_o = 76.2$ mm
For smooth tubes:		0.80	0.82
For k = 0.25 mm:	2.0	0.85	0.91
	5.0	1.03	1.03
	10.0	1.10-0.85	1.11-0.80
For k = 0.51 mm:	2.0	0.83	0.89

The rough surface with  $p/k = 10$  shows a maximum increase in Nusselts number. Fig. 23 shows a plot of  $Nu/Nu_0$  against  $k/\delta_L$ . The nature of the curve confirms speculations of Sheriff & Edward (12) that at  $k/\delta_L > 8$  the rough elements are fully effective.

## 8. Heat transfer and friction factor - experimental data for

### WATER

#### 8.1. Circular tube with sand-grain type roughness and and commercial pipes (air)

Experiments conducted by Dipprey (8) can be regarded as essentially an extension of the classical experiments of Nikuradse (27) with sand-grain type roughness. Data were collected for distilled water flowing vertically upwards through a pipe of 102 mm nominal inner diameter. Inner surface of the tube was roughened. Prandtl's number range covered was from 1.20 to 5.94. Reynolds number range covered was from  $1.4 \cdot 10^4$  to  $5.2 \cdot 10^5$ .

The pipe roughness was characterised by the length "h" which is equivalent sand roughness height. Three rough tubes were tested. Their effective roughness ratios were:

$h/D$   
0.0488  
0.0138  
0.0024

The plot of friction factor vs. Reynolds number at constant Prandtl's number have an usual descending characteristics upto a point. After passing through a minimum friction factor becomes independent of Reynolds number.

The plot of Stanton number vs. Reynolds number at constant Prandtl's number passes through a maxima in the transition region (i. e. , before the flow becomes fully rough). Thereafter, Stanton number decreases slowly with increasing Reynolds number.

Two graphs (fig. 24 & fig. 25) reproduced show  $\frac{8St}{f}$  plotted against Reynolds number. Dipprey concludes that at low Prandtl's numbers ( $Pr < 3$ ) the  $\frac{8St}{f}$  values can only be lowered by roughening the heat transfer surface. At higher Prandtl's numbers, however, it is possible to have higher values of  $\frac{8St}{f}$  than a smooth tube.

#### Commercial pipes

Smith and Epstein (37) investigated the effect of wall roughness on coefficient of heat transfer and friction factor in six commercial pipes. The tests covered a  $D/h$  ratio of 64 to 640. The Reynolds number range covered was from  $10^4$  to  $8 \cdot 10^4$ . Galvanized and standard steel pipes gave rise to similar variations in  $St \cdot Pr_f^{2/3}$  when plotted against  $Re_f$  (see fig. 26). The equation of Boelter, Martinelli and Jonassen (eqn.12) was reduced to the following form assuming  $D. R. = 1$  and  $Pr_f = 0.69$  for air:

$$\frac{\sqrt{f_f/4}}{St \cdot Pr_f^{2/3}} = 10.425 \log Re_f \sqrt{f_f/4} - 0.3395$$

Fig. 27 shows a plot of  $\sqrt{f_f/4} St \cdot Pr_f^{2/3}$  against  $\log Re_f \sqrt{f_f/4}$ . At higher Reynolds numbers the agreement between the theoretical equation and the experimental data is quite good. Smith and Epstein feels that if  $\Delta t_{max}/\Delta t_{mean}$  and  $D. R.$  are properly evaluated then at lower Reynolds number the scatter of the data will decrease.

8.2. Annular channel with inner tube roughened

An annular configuration with the inner tube roughened was tested by Kemeny and Cyphers (20). Roughness elements were semi-circular type. Both integral and attached type of protrusions were tested. A third type which consisted of spiral groove was also tested. Average height or depth of roughness elements was 0.13 mm. Two p/k ratios of 10 and 20 were investigated. The annulus had following dimensions:  $d_o = 17.483$  mm and  $d_i = 12.7$  mm.

Different roughness elements tested were as follows:

Roughness height k (average) mm	Pitch to height ratio p/k	Designation in ref. 20	Description
0		Smooth	Smooth tube
0.117	10	P & W 10-1	Integral spiral thread
0.124	20	P & W 20-1	Integral spiral thread of semi-circular cross-section with 0.013 mm groove machined between 0.124 mm roughness elements
0.135	10	W 10 - 1 w	0.254 mm diameter wire wound into 0.127 mm groove
0.132 (depth)	10	W 10 - 1 g	0.132 mm deep groove without wire

Nusselts number plotted against Reynolds number for different types of roughness elements (see fig. 28) indicates that at lower Reynolds numbers the values for the grooved tubes are the same as that for the smooth tubes. Brauer (2), however, found

that the grooved tubes gave lower Nusselts number than smooth tubes at lower Reynolds numbers.

In the fig. 29 pressure drop per unit length is plotted against Nusselts numbers. It indicates that the integral spiral threaded type of roughness elements are superior to other types. The wire-wound type has the same profile as the spiral threads but they give lower coefficients of heat transfer. Because the thermal resistance at the contact point between the wire and the tube surface is quite high.

A relation between Stanton number and friction factor can be written in the following way:

$$\frac{St}{f \cdot G} = C \cdot \frac{\alpha}{\Delta P} \quad (36)$$

where,  $C = \frac{A_w}{8 A_c \cdot C_p \cdot \rho}$

For a given physical configuration "C" is constant. The fig. 30 in which  $4St/f \cdot G$  is plotted against bulk Reynolds number shows that the grooved tube (designated as W 10 - 1 g) has the highest relative efficiency over practically the whole range of Reynolds numbers. The fig. 29, however, indicates that the integral spiral type is better than other types. It seems that conclusions drawn on the basis of  $St/f \cdot G$  vs.  $Re$  diagram might be misleading.

Using Nunner's data Kemeny and Cyphers (20) obtained the following empirical relation for calculating the friction factor for a roughened tube. In the following equation "f" is the friction factor when the roughness elements extend over the whole wetted perimeter.

$$f/f_o = 4 \text{ Re}^{0.3} k/d_H \left[ 7.50 - 2.63 (\ln 10 k/p)^{8/5} \right] \quad (37)$$

By substituting Blassius law for  $f_o$  in the above equation one obtains:

$$f = 4 \text{ Re}^{0.05} k/d_H \left[ 0.593 - 0.0208 (\ln 10 k/p)^{8/5} \right] \quad (38)$$

If a part of the wetted perimeter is roughened then the friction factor can be modified in the following way:

$$f_{\text{modified}} = C_o (f - f_o) + f_o \quad (39)$$

where,  $C_o$  is the fraction of the area roughened.

Kemeny and Cyphers suggested that their experimental data together with Nunner's data can be approximated by Martinelli's equation for heat transfer (24). Martinelli (24) correlated Cope's (5) data on rough tubes by the following equation:

$$\text{Nu} \sqrt{\text{Pr}} = \frac{1.04 \text{ Re} \cdot \text{Pr} \cdot f/8}{14.5 + \ln(\text{Re} \cdot \text{Pr} \cdot f/8)} \quad (40)$$

The fig. 31 reproduced from ref. 24 indicates close correspondence between the equation and data from Cope's experiments (4). Fig. 32 & 33 from ref. 20 shows that data of Nunner as well as that of Kemeny and Cyphers agree rather well with the equation. This is definitely remarkable because Nunner's theoretical equation gave a rather poor agreement with data obtained by others (2) (21) for water.

Brauer (2) studied the effect of roughened inner tubes on heat transfer in annuli. The heat transfer medium was water. Roughness were of integral type, ribs of very small height "k" spaced

at varying distances "a" and grooves. Reynolds number range covered was from  $2 \cdot 10^2$  to  $10^5$ . The distance "a" between the roughness elements were varied from 0.3 mm to 20 mm. Height of the roughness elements were constant at  $k = 0.3$  mm. Two ratios of external diameter ( $d_o$ ) to internal diameter ( $d_i$ ) were tested. They were as follows:

$d_o$	$d_i$	$d_o/d_i$
mm	mm	
19	15	1.287
19.3	11	1.728

The theoretical frictional law for laminar flow through a concentric annulus which has been used in calculating "f" for smooth tubes is as follows:

$$f = C \cdot \frac{64}{Re} \quad (41)$$

where, "C" is as follows:

$$C = \frac{(d_o/d_i - 1)^2 \ln d_o/d_i}{(d_o^2/d_i^2 + 1) \ln d_o/d_i - (d_o^2/d_i^2 - 1)}$$

The hydraulic diameter " $d_H$ " is given by:

$$d_H = \frac{4 A_c}{A_w} = d_o - d_i \quad (42)$$

" $d_H$ " is used as the characteristic length in the Reynolds number. When the inner tube is ribbed the modified hydraulic diameter " $d_H$ " can be written in the following form:

$$d_{H'} = d_o \frac{1 - (d_i/d_o)^2 (1 + 4 b/p [k/d_i + (k/d_i)^2])}{1 + (d_i/d_o) (1 + 2 k/p [1 + k + b/d_i])} \quad (43)$$

replacing  $d_o - d_i$  by  $d_H$  we get:

$$\frac{d_{H'}}{d_H} = \frac{1 + 4 b/p [k/d_i + (k/d_i)^2]}{1 + 2 k/p [1 + k + b/d_i]} \quad (44)$$

Experimental results indicated, naturally, that the values of friction factor for annular sections with roughened tubes lie higher than those for smooth annular channels. It was found difficult to establish any interrelationship between the geometrical factors and friction factor in the laminar range. However, individual roughness elements gave a  $f$  vs  $Re$  relationship which was more or less parallel to the smooth tube curve. The following table is quoted from ref.

Rib distance "a" in mm	Spacing ratio $p/b$	Friction factor ratio $f/f_o$
0.3	2.00	2.00
0.6	3.00	2.00
1.2	5.00	2.00
2.6	9.67	2.00
5.2	18.33	1.37
10.1	34.87	1.14
20.1	68.00	1.05

In the turbulent region the friction factor, it is mentioned, could be correlated by an equation of the following form:

$$f = C \cdot Re^n \quad (45)$$

where,  $n = 0.1$ .

But "C" turned out to be different for different geometries. With increasing "a" it passes a maxima with  $a = 2.6$  mm and decreases thereafter.

Unlike the ribbed surfaces the grooved surfaces did not affect the friction factor in the laminar range. As an explanation Brauer (2) suggests that the grooves are filled with stagnant viscous boundary layer which does not influence the flow near the wall.

With changing  $d_o/d_i$  ratio the exponent "n" in the equation  $f = C \cdot Re^n$  changed:

	$d_o/d_i$	n
Circular tube		0.25
Annulus	1.728	0.25
Annulus	1.287	0.17
Annulus	1.000	0.00

Heat transfer curves (Nu vs. Re) for grooved roughness elements show that at the laminar flow region the Nusselts number lies below that for the smooth-walled annulus. A possible explanation to this is that the grooved pits are filled with viscous boundary layer mass. This gives rise to increased resistance to heat flow.

With ribbed roughness the transition to well-developed turbulent flow is quicker with smaller distance between the ribs. Spacing ratio is defined as

$$\frac{\text{pitch}}{\text{width of roughness in the flow direction}} = \frac{p}{b}$$

Referring to fig. 34, 35 & 36 one notices that with  $p/b$  ratio  $f/f_o$  increases until at about  $p/b = 8$  it reaches a maximum and then

decreases. The nature of the curve are the same in wide and narrow channels. But the actual values of  $f/f_o$  are much higher for narrow channels. This suggests that a ratio of the nature of  $k/d_H$  should also be taken into account. Lancet (21) had found in his experiment that for an extremely narrow channel even a smooth tube with fine scratches on it behave as if it is a rough surface.

$Nu/Nu_o$  vs.  $Re$  curves also show the same tendency of having a maxima at  $p/b$  ratio of 8. The magnitude of  $(Nu/Nu_o)_{max}$  at the same Reynolds number is substantially constant for different annulus. This indicates that the effect of  $k/d_H$  ratio is sharper on  $f/f_o$  than on  $Nu/Nu_o$ . (See fig. 37, 38, 39, 40 & 41). The theoretical equation for heat transfer in roughened tubes given by Nunner (28) can be modified in the following form:

$$A = \frac{1.0 + 1.5 Re^{-1/8} \cdot Pr^{-1/6} (Pr - 1)}{1.0 + 1.5 Re^{-1/8} \cdot Pr^{-1/6} (Pr \cdot \frac{f}{f_o} - 1)}$$

$$Nu/Nu_o = A \cdot f/f_o \quad (46)$$

for  $f/f_o > 1$   $A$  is always less than 1.

So, if  $Nu/Nu_o$  is plotted against  $f/f_o$  then according to the theory all values should lie below the straight line represented by  $Nu/Nu_o = f/f_o$ . However, the experimental data indicates that such is not the case always. If the Nusselts number is modified by taking into account the increase in the heat transfer area due to roughness then all the values lie below the  $Nu/Nu_o = f/f_o$  straight line. Qualitatively, thus, some agreement is obtained with Nunner's theory but the quantitative agreement is poor. Brauer suggests that Nunner's theory is derived on the assumption that the roughness is limited essentially to the region of the

viscous wall layer. But in Brauer's experiment the roughness elements protrude well beyond the viscous wall layer.

## 9. Friction factor

### 9.1. Circular tube with drilled holes as roughness elements

Pressure drop data for water flowing through two roughened tubes of nominal diameters 0.9 cm and 1.6 cm were collected by O'Sullivan (29). Here the roughness elements were of the form of drilled holes of equal depth at regular distances. Smooth pipe data were correlated in this experiment as:

$$\begin{aligned} f &= 0.3176/Re^{0.25} && \text{for } d = 0.9 \text{ cm} \\ f &= 0.3404/Re^{0.25} && \text{for } d = 1.6 \text{ cm} \end{aligned}$$

In the laminar flow range the holes do not affect the friction factor. Referring to fig. 42 one notices that at higher Reynolds numbers the curves for the roughened tubes tend to become parallel to the smooth tube curve. In the fig. 43 in which  $f/f_0$  is plotted against  $Re$  this tendency is noticed more clearly. The above findings agree qualitatively with Brauer's findings for grooved tubes.

Brauer's results indicated that for grooved tubes above  $Re = 10^4$   $f$  is more or less constant. But in fig. 42 one notices that above  $Re = 10^4$   $f$  starts decreasing.

The data obtained indicates that friction factor is affected by the various geometrical factors like depth, diameter and pitch of the holes. From the information available no quantitative assessment is possible.

### 9.2. Annular channel with inner tube roughened

Durant (11) studied the effect of medium diamond knurls (approximately 37 points per sq. cm.) on friction factor in an

annulus with the inner wall roughened with such a roughness. Outer diameter of the inner tube is 12.7 mm.

Durant correlates his experimental data with the following equation:

$$\frac{1}{\sqrt{f}} = Re^{0.14} \cdot \ln \sqrt{\frac{d_H}{k}} + \frac{29}{Re} 0.20 \quad (47)$$

Experimental limits of the above equation are:

Type of roughness	medium diamond knurls
Depth of roughness	$k = 0.18 \text{ mm to } 0.41 \text{ mm}$
Equivalent diameter	$d_H = 7.37 \text{ mm to } 12.95 \text{ mm}$
Reynolds number	$Re = 10^5 \text{ to } 2.5 \cdot 10^5$
Per cent of wetted perimeter roughened	33 % to 39 %
Medium	water

Fig. 44 shows a plot of the equation 47. Scatter of the data is less than 10 %.

#### 10. Transformation of experimental data

From the data already presented it is quite evident that heat transfer and pressure drop data for roughened surfaces are quite often obtained in annular passages with the inner surface roughened. To apply these data to a system which differs in the following three respects certain modifications are required.

1. the shape of the two systems are different.
2. the proportion of rough to smooth surface is different.
3. the proportion of heated to unheated surface is different.

A transformation is suggested by Hall (17) in an attempt to reduce the data to a form in which they are directly comparable with a system having the whole of the surface heated and roughened. The use of the hydraulic diameter takes care of the change in shape.

The steps in the transformation is as follows:

1. From the experimental velocity distribution the radius " $r_m$ " at which  $\frac{du}{dr} = 0$  is obtained.
2.  $d_H$  and  $d_{H_1}$  are calculated from the following relations.

$$d_{H_1} = \frac{4\pi [r_m^2 - r_i^2]}{2\pi r_i} \quad (48)$$

$$d_H = \frac{4\pi [r_o^2 - r_i^2]}{2\pi(r_i + r_o)} \quad (49)$$

3.  $f_{mod}$  is given by

$$\frac{f_{mod}}{f} = \frac{\int_{r_i}^{r_o} \rho \cdot u \cdot r \cdot dr}{\int_{r_i}^{r_m} \rho \cdot u \cdot r \cdot dr} \cdot \frac{\int_{r_i}^{r_o} u \cdot r \cdot dr}{\int_{r_i}^{r_m} u \cdot r \cdot dr} \cdot \frac{d_{H_1}}{d_H} \cdot \left[ \frac{A_{im}}{A_{io}} \right]^2 \quad (50)$$

4. Modified Reynolds number is given by

$$\frac{Re_{mod}}{Re} = \frac{\int_{r_i}^{r_m} u \cdot r \cdot dr \cdot A_{io} \cdot d_{H_1} \cdot \mu}{\int_{r_i}^{r_o} u \cdot r \cdot dr \cdot A_{im} \cdot d_H \cdot \mu_1} \quad (51)$$

5. The modified radial temperature gradient at  $r$  is given by,

$$\left(\frac{\delta t}{\delta r}\right)_{\text{mod}} = \frac{\delta t}{\delta r} \cdot \frac{\int_{r_i}^{r_o} \rho \cdot u \cdot r \cdot dr \cdot \int_r^{r_m} \rho \cdot u \cdot r \cdot dr}{\int_{r_i}^{r_m} \rho \cdot u \cdot r \cdot dr \cdot \int_r^{r_o} \rho \cdot u \cdot r \cdot dr} \quad (52)$$

6.  $\Delta t$  and  $(\Delta t)_{ib}$  are determined from the experimental and modified temperature distributions respectively.

7. Modified Stanton number is obtained as follows:

$$\frac{St_{\text{mod}}}{St} = \frac{(\Delta t)_{\text{mean}}}{(\Delta t)_{ib}} \cdot \frac{m_{io}}{A_{io}} \frac{A_{im}}{m_{im}} \quad (53)$$

Fig. 45 & 46 are reproduced from ref. 17 to clarify the transformation to a certain extent.

Walker (39) mentions that Hall's method helps in predicting pressure loss measurements made in 21 rod clusters with two different types of roughness elements to better than 10 %.

Results obtained by the transformation described above is slightly complicated because with similar flow parameters but with different roughness elements different Reynolds numbers are obtained.

## 11. Practical application

Heat transfer  $Q$  across a surface area  $H$  is given by

$$Q = \alpha \cdot \Delta t_m \cdot H \quad (54)$$

Pumping power  $N$  needed to pump a volume " $V$ " through a heat exchanger is given by:

$$N = V \cdot \Delta P \quad (55)$$

For maximum heat transfer with minimum energy loss  $Q/N$  ratio should be as high as possible. For a particular configuration with a particular surface roughness,  $H$  is a function of  $\epsilon = Q/N$ . For  $Q = 1000$  Kcal/h and  $\Delta t_m = 1$  °C the  $Q/N$  factor is denoted as  $\epsilon_1$  and it is called a "performance factor".

As examples two figures are reproduced from ref. 2. In these  $\epsilon_1$  is plotted against  $H$  for different kinds of roughness elements in some particular annuli. Choosing a value of  $\epsilon_1$  one can find out the area  $H$  required to transmit 1000 Kcal/h at a mean temperature difference of 1 °C. Then the area  $H_2$  required to transmit  $Q_2$  Kcal/h at a temperature difference of  $t_m$  °C is given by

$$\frac{H_2}{H} = \frac{Q_2}{1000} \cdot \frac{1}{\Delta t_m} \quad (56)$$

The fig. 47 indicates that for this particular annulus at lower values of  $\epsilon_1$  rough tubes help in reducing the necessary heat transfer area but at higher values smooth tubes give a better performance. The fig. 48 on the other hand shows an opposite tendency. So it is not self-evident that roughness elements always helps in reducing the necessary heat transfer area.

#### Acknowledgement

The author takes this opportunity of thanking Prof. T. Widell of Royal Institute of Technology, Stockholm, Mr. J. Flinta of Heat Laboratory of AB Atomenergi and Prof. G. Tyllered of Lund Institute of Technology for their kind help.

List of notations

Capital letters

A	empirical constant
$A_c$	area of flow cross-section
$A_{im}$	cross sectional area of the passage bounded by $r_i$ and $r_m$
$A_{io}$	cross sectional area of the passage bounded by $r_i$ and $r_o$
$A_w$	wetted area for unit length of channel
$A [K^*]$	friction similarity function, defined by eqn. 8
B	empirical constant from eqn. 8
$C_o$	fraction of area roughened
$C_p$	specific heat at constant pressure
D	diameter
E	empirical constant from eqn. 8
DR	diffusivity ratio $\frac{E_H}{E_H + \lambda/\rho \cdot c_p}$
$E_H$	eddy diffusivity of heat
G	mass flow velocity = $\rho w$
$H_2, H_1$	heat transfer area
$K^*$	dimensionless roughness height = $\frac{K v^*}{\nu}$
$K_f$	empirical constant from eqn. 10
L	length
N	pumping power
Q	heat transfer across an area H (eqn. 54)
$T_b$	average bulk temperature of fluid
$T_f$	film temperature = $\frac{T_b + T_s}{2}$
$T_h$	mean temperature of the fluid at the outer edge of the sub-layer
$T_s$	temperature of the solid surface
V	volume

Italics

- a distance between roughness elements =  $p - b$
- b width of roughness elements
- $d_i$  inner diameter of an annulus
- $d_H$  equivalent diameter =  $\frac{4A_c}{A_w}$
- $d_{H_1}$  equivalent diameter of passage bounded by  $r_i$  and  $r_m$  neglecting the wetted surface at  $r_m$
- $d_M$  mean diameter defined by eqn. 23
- $d_o$  outer diameter of an annulus
- f friction factor as defined in eqn. 1
- $g[K^* \cdot Pr]$  dimensionless heat transfer similarity function defined by eqn. 9
- h effective thickness of layer associated with roughness or equivalent sand roughness
- k height of roughness elements
- m exponent
- $m_{im}$  mass flow in the passage bounded by  $r_i$  and  $r_m$
- $m_{io}$  mass flow in the passage bounded by  $r_i$  and  $r_o$
- n exponent
- p pitch of roughness elements
- q rate of heat transfer across unit area
- r radius
- $r_i$  inner radius of an annulus
- $r_m$  radius at which  $\frac{du}{dr} = 0$
- $r_o$  outer radius of an annulus
- s clear peripheral spacing between elements

- $t_s$  temperature of the solid surface in  $^{\circ}\text{C}$
- $w$  mean fluid velocity
- $v_*$  friction velocity =  $w \sqrt{f/8}$
- $(\Delta t)_{ib}$  temperature difference between inside surface of a channel and bulk of fluid based on modified temperature distribution
- $\Delta t_m$  mean temperature difference (eqn. 54)
- $\Delta t_{\text{mean}}$  temperature difference between inside surface of pipe and bulk of fluid
- $\Delta t_{\text{max}}$  temperature difference between inside surface of pipe and axis of pipe

Greek letters

- $\rho$  fluid density
- $\mu$  fluid viscosity
- $\nu$  fluid Kinematic viscosity =  $\frac{\mu}{\rho}$
- $\delta_L$  thickness of laminar sub-layer
- $\delta_B$  combined thicknesses of laminar sub-layer and buffer layer
- $\lambda$  thermal conductivity of fluid
- $\gamma$  ratio of specific heat at constant pressure to specific heat at constant volume
- $\alpha$  coefficient of heat transfer
- $\mu_1$  viscosity at the bulk mean temperature of that portion of the whole flow which passes through the annulus from  $r_i$  to  $r_m$
- $\epsilon = Q/N$
- $\epsilon_1$  performance factor  $Q/N$  for  $Q = 1000 \text{ Kcal/h}$  and  $\Delta t_m = 1^{\circ}\text{C}$

Dimensionless numbers

- Re Reynolds number  $\frac{G \cdot D}{\mu}$

St	Stanton number	$\frac{\alpha}{\rho w C_p}$
Nu	Nusselts number	$\frac{\alpha D}{\lambda}$
Pr	Prandtls number	$\frac{\mu C_p}{\lambda}$
M	Mach number	$u/\sqrt{\gamma RT}$

Rest

$\frac{dP}{dL}$  pressure gradient in the direction of flow

$\Delta P$  pressure drop

$\frac{\delta t}{\delta r}$  temperature gradient in the radial direction

Subscripts

FR fully rough

sub sub-layer

f or film film, fluid properties evaluated at temperature  $T_{\text{film}}$

o smooth tube valves

mod modified

s surface, fluid properties evaluated at temperature  $T_s$

b bulk, fluid properties evaluated at temperature  $T_b$

max maximum

References

1. BOELTER L M K, MARTINELLI R C and JONASSEN F  
Remarks on the analogy between heat transfer and momentum transfer.  
Trans. ASME., 63, 447-455, 1941.
2. BRAUER H  
Flow resistance and heat transfer in annuli with roughened inner tubes.  
Mannesmann Forschungsberichte 109/1961.  
(Translated by Chillag J P, Australian Atomic Energy Commissions Research Establishment, Lucas Heights)  
AAEC/Trans. 13.
3. BURNETT P and HORN G  
The heat transfer properties of rough surfaces.  
UKAEA IGR-TN/W-1008, 1959. 2)
4. COPE W F  
The friction and heat transmission coefficients.  
Inst. of Mech. Engr. Proc., Vol. 137, pp 165, 1937.
5. COPE W F  
The friction and heat transmission coefficients of rough pipes.  
Inst. of Mech. Engr. Proc., Vol. 145, pp 99, 1941.
6. DEISSLER R G  
Analytical investigation of turbulent flow in smooth tubes with heat transfer with variable fluid properties for Prandtl number of 1.  
NACA Technical Note 2242, 1950.
7. DEISSLER R G and EIAN C S  
Analytical and experimental investigation of fully developed turbulent flow of air in a smooth tube with heat transfer with variable fluid properties.  
NACA Technical Note 2629, 1952.
8. DIPPREY D F and SABERSKY R H  
Heat and momentum transfer in smooth and rough tubes at various Prandtl numbers.  
Technical Report N 32-269  
Jet Propulsion Laboratory  
California Institute of Technology, Pasadena, U.S. A., 1962.

---

2) No material has been taken from ref. 3 and ref. 41 in preparing this literature survey.

9. DONNE M DALLE and BOWDITCH F H  
High temperature heat transfer, local heat transfer and average friction coefficients for subsonic laminar, transitional and turbulent flow of air in a tube at high temperature. Nuclear Engineering, Vol. 8, No. 80, pp 20, 1963.
10. DRAYCOTT A and LAWTHORP K R  
Improvement of fuel element heat transfer by use of roughened surfaces and the application to a 7-rod cluster. International Developments in Heat Transfer, ASME, Part III, 1961.
11. DURANT W S  
Friction factors for flow of water in an annulus with one roughened wall.  
DP-583 (Reactor Technology TID-4500 16th Ed.), 1961.
12. EDWARDS F J and SHERIFF N  
The heat transfer and friction characteristics for forced convection air-flow over a particular type of rough surface. International Developments in heat transfer, ASME, Part II, 1961.
13. FOURNEL E  
On a method of improving heat exchange by forced convection. AERE Lib/Trans. 659, 1952.
14. GIJNEN W H  
Principles of engineering heat transfer.  
D Van Nostrand, Co. Inc., New York, N. Y., pp 181, 1957.
15. GOLDSTEIN S  
A note on roughness.  
ARC R & M 1763, 1936.
16. GRASS G  
The improvement of heat transfer to water derivable from the artificial roughening of surfaces in reactors.  
AEC TR-3641.  
(from Atomkernenergie 3, 328-31 (1950)).
17. HALL W B  
Heat transfer in channels composed of rough and smooth surfaces.  
U. K. A. E. A. Industrial Group, IGR-TN/W-832, 1958.
18. HOFMANN E  
The general law of heat transfer for turbulent flow in tubes and the significance of the characteristic numbers.  
AERE Lib/Trans. 674 (From "Forschung auf dem Gebiete des Ingenieurwesens", 20, No. 3, pp 81-93, 1954).

19. von KÁRMÁN Th  
The analogy between fluid friction and heat transfer.  
Trans. ASME, Vol. 61, pp 705, 1939.
20. KEMENY G A and CYPHERS J A  
Heat transfer and pressure drop in an annular gap with  
surface spoilers.  
Trans. ASME. Ser. C. Vol. 83, No. 2, pp 189, 1961.
20. a KREITH F and MARGOLIS D  
Heat transfer and friction in turbulent vortex flow.  
Applied Scientific Research, sec A.  
Vol. 8, pp 457, 1959.
21. LANCET R T  
The effect of surface roughness on the convection heat-  
transfer coefficient for fully developed turbulent flow in  
ducts with uniform heat flux.  
Trans. ASME, Journal of Heat Transfer, Vol. 81, Ser. C,  
No. 2, pp 168, 1959.
21. a LIEPMANN H W and FILA G H  
Investigations of effects of surface temperature and single  
roughness elements on boundary-layer transition.  
NACA Report No. 890, 1946.
22. LOGAN Jr EARL  
Effects of a change in wall roughness on fully developed  
flow in a circular pipe.  
Purdue University, Ph. D. Thesis, 1961.
23. LOHRENZ J and KURATA F  
A friction factor plot for smooth circular conduits, con-  
centric annuli and parallel plates.  
Ind. & Eng. Chem., Vol. 52, No. pp 703, 1960.
24. MARTINELLI R C  
Heat transfer to molten metals.  
Trans. ASME, Vol. 69, No. 11, pp 947, 1947.
25. MATTIOLI G D  
Theory der Wärmeübertragung in Glatten und Rauhen Rohren.  
Forschung auf dem Gebiete des Ingenieurwesens, Ausgabe A,  
Band II No. 4, July-Aug. pp 149-158, 1940.  
(Translation: NACA Technical Memorandum 1037).
26. MORRIS H M  
Flow in rough conduits.  
Transactions of the American Society of Civil Engineers,  
Vol. 120, No. 2745, pp 373-410, 1955.

27. NIKURADSE J  
Stromungsgesetze in rauhen Rohren.  
VDI-Forschungsheft 361. Beilage zu "Forschung auf dem  
Gebiete des Ingenieurwesens",  
Ausgabe B, Band 4, July/August 1933.  
(Translation: NACA Technical Memorandum 1292, 1950).
28. NUNNER W  
Heat transfer and pressure drop in rough tubes.  
AERE Lib/Trans. 786 (From VDI Forschungsheft 455,  
Supplement to "Forschung auf dem Gebiete des Ingenieur-  
wesens" B, Vol. 22, pp 5, 1956).
29. O'SULLIVAN J K  
Flow in pipes with drilled holes. (Effects similar to sur-  
face waviness).  
Engineering, Vol. 183, No. 4760, pp 684, 1957.
30. OWEN P R and THOMSON W R  
Heat transfer across rough surfaces.  
Journal of Fluid Mechanics, Vol. 15, Part 3, 1963.
31. PINKEL B  
A summary of NACA research on heat transfer and friction  
for air flowing through a tube with large temperature  
difference.  
Trans. ASME., Vol. 76, No. 2, pp 305, 1954.
32. SAMS E W  
Heat transfer and pressure drop characteristics of wire-  
-coil type turbulence promoters.  
Reactor Heat Transfer Conference of 1956, United States  
Atomic Energy Commission Technical Information Service  
Extension, Oak Ridge, Tenn., TID-7529 (Pt. 1) Book 2,  
pp 390, 1957.
33. SAMS E W  
Experimental investigation of average heat transfer and  
friction coefficients for air flowing in circular tubes  
having square-thread type of roughness.  
NACA RM E52 D 17, 1952.
34. SCHLICHTING H  
Boundary layer theory.  
McGraw-Hill Book Company, Inc., New York, 1960.
35. SHERIFF N, GUMLEY P and FRANCE J  
Heat transfer characteristics of roughened surfaces.  
UKAEA, TRG Report 447 (R), 1963.

36. SMITH J C  
Fluid friction and heat transfer in cylindrical pipes,  
relationship between lumped and distributed parameters.  
The Canadian Journal of Chemical Engineering, June,  
pp 106, 1961.
37. SMITH J W and EPSTEIN N  
Effect of wall roughness on convective heat transfer in  
commercial pipes.  
AIChE Journal, Vol. 3, No. 2, pp 241, 1957.
38. TANI J, HAMA R and MITUSI S  
On the permissible roughness in the laminar boundary  
layer.  
Aero. Res. Inst. Tokyo, 199, 1940.
39. WALKER V  
The improvement of fuel element heat transfer by surface  
roughening.  
Nuclear Engineering, April, pp 144, 1961.
40. WALKER V and RAPIER A C  
Fuel element heat transfer.  
The Journal of British Nuclear Energy Society, Vol. 2,  
No. 2, pp 268, 1963.
41. WILKIE D and WILSON J T  
Pressure drop tests on 21-rod smooth and roughened  
clusters.  
UKAEA, TRG Report 29 (W), 1961. 3)
42. MELESE G B  
Comparison of partial roughening of the surface of fuel  
elements with other ways of improving performance of  
gas-cooled Nuclear Reactors  
GA-4624, 1963.
43. MELESE G B  
Improvement in thermal performance of a Nuclear  
Reactor by local changes in surface heat transfer  
properties  
GA-4619, 1963.
44. MALHERBE T  
Influence des rugosités de paroi sur les coefficients  
d'échange thermique et de perte de charge  
Rapport C. E. A. N° 2283, 1963

---

3) See footnote 2, page 50.

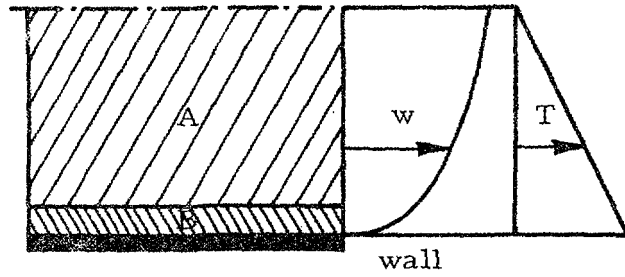


Fig. 1. Velocity profile in a smooth tube

- A - turbulent core
- B - viscous wall layer
- w - local velocity
- T - local shearing stress

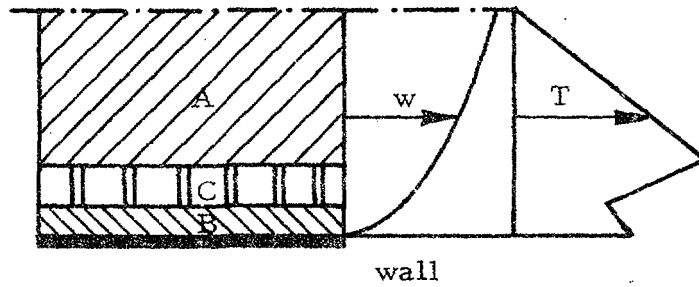


Fig. 2: Velocity profile in a rough tube

- A - turbulent core
- B - viscous wall layer
- C - roughness zone
- w - local velocity
- T - local shearing stress

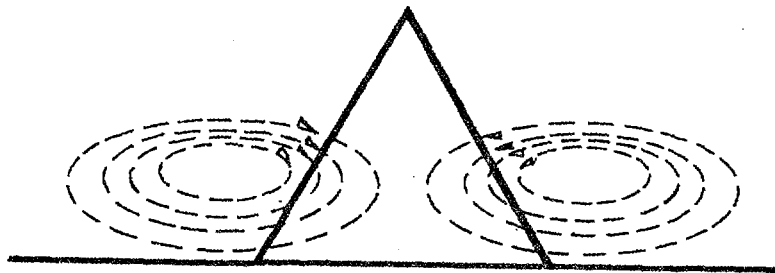


Fig. 3. Rough sketch of the horseshoe eddies behind an excrescence.

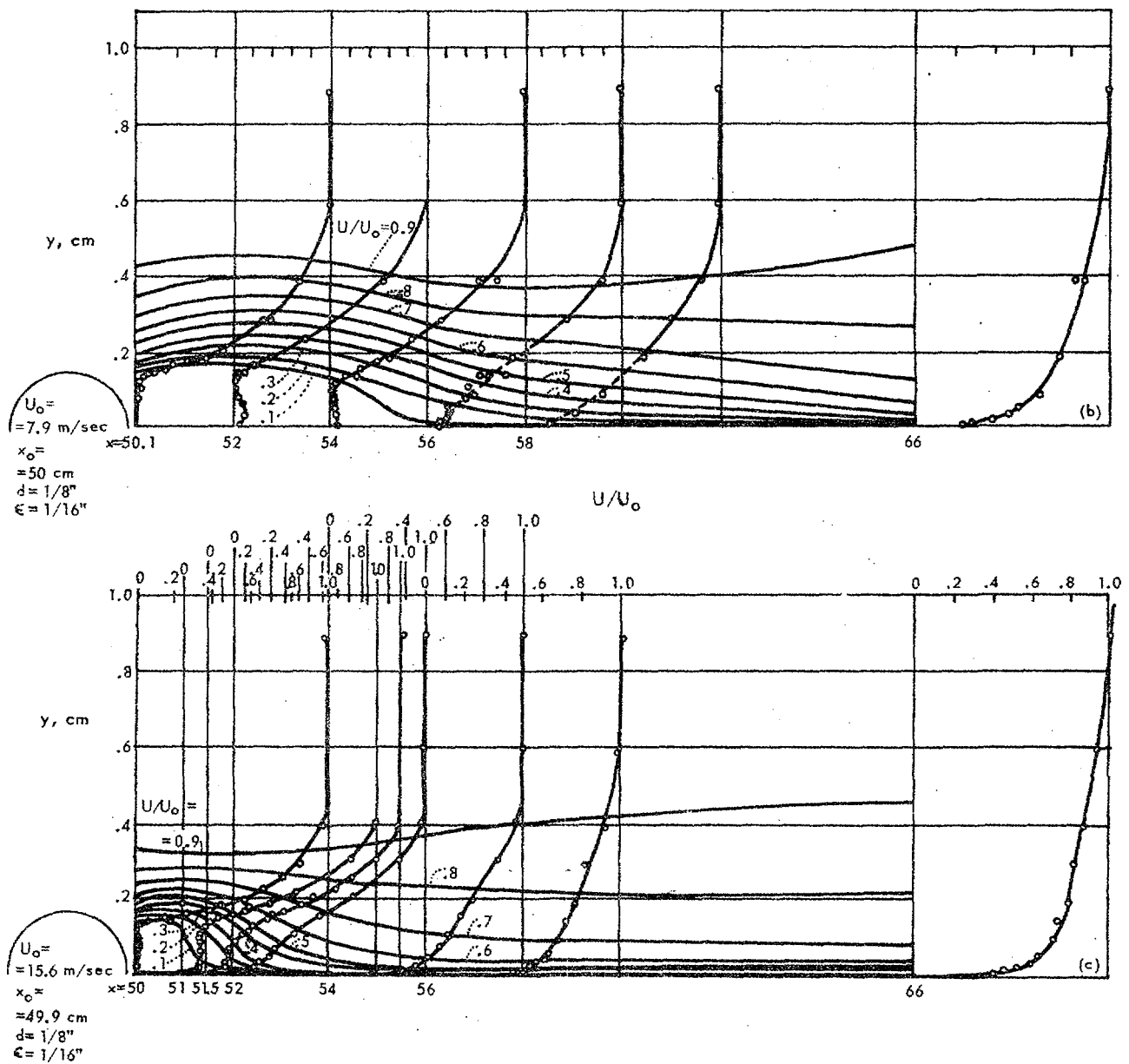


Fig. 4. Velocity profiles downstream from a small roughness element.

- $x$  = distance along surface of plate from leading edge
- $y$  = distance perpendicular from surface of plate
- $x_0$  = distance of roughness element from leading edge of plate
- $U^0$  = local mean velocity in the  $x$  direction
- $U_0$  = mean velocity of free stream in  $x$  direction
- $d$  = diameter of the two dimensional roughness
- $\epsilon$  = height of roughness element.

No	item	dimensions	D (cm)	d (cm)	k (cm)	k <sub>s</sub> (cm)	photographs
1	spheres		4	0.41	0.41	0.093	
2			2	0.41	0.41	0.344	
3			1	0.41	0.41	1.26	
4			0.6	0.41	0.41	1.56	
5			densest arrgt.	0.41	0.41	0.257	
6			1	0.21	0.21	0.172	
7			0.5	0.21	0.21	0.759	
8	spherical segments		4	0.8	0.26	0.031	
9			3	0.8	0.26	0.049	
10			2	0.8	0.26	0.149	
11	cones		densest arrgt.	0.8	0.26	0.365	
12			4	0.8	0.375	0.059	
13			3	0.8	0.375	0.164	
14			2	0.8	0.375	0.374	
15	"short" angles		4	0.8	0.30	0.291	
16			3	0.8	0.30	0.618	
17			2	0.8	0.30	1.47	

Fig. 5. Results of measurements on regular roughness patterns,

k = actual height of protrusion

k<sub>s</sub> = equivalent sand roughness = (h)

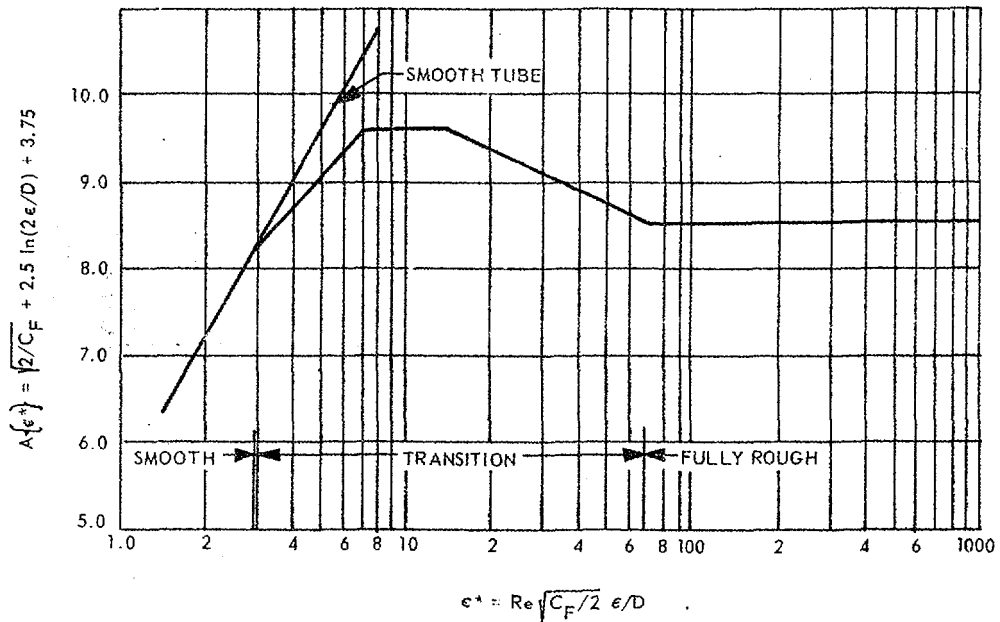


Fig. 6. Friction similarity function for closed-packed sand-grain roughness.

abscissa -  $K^* = \text{Re} \cdot \left[ \frac{f}{8} \right]^{1/2} \cdot \frac{k}{D}$

ordinate -  $A[K^*]$

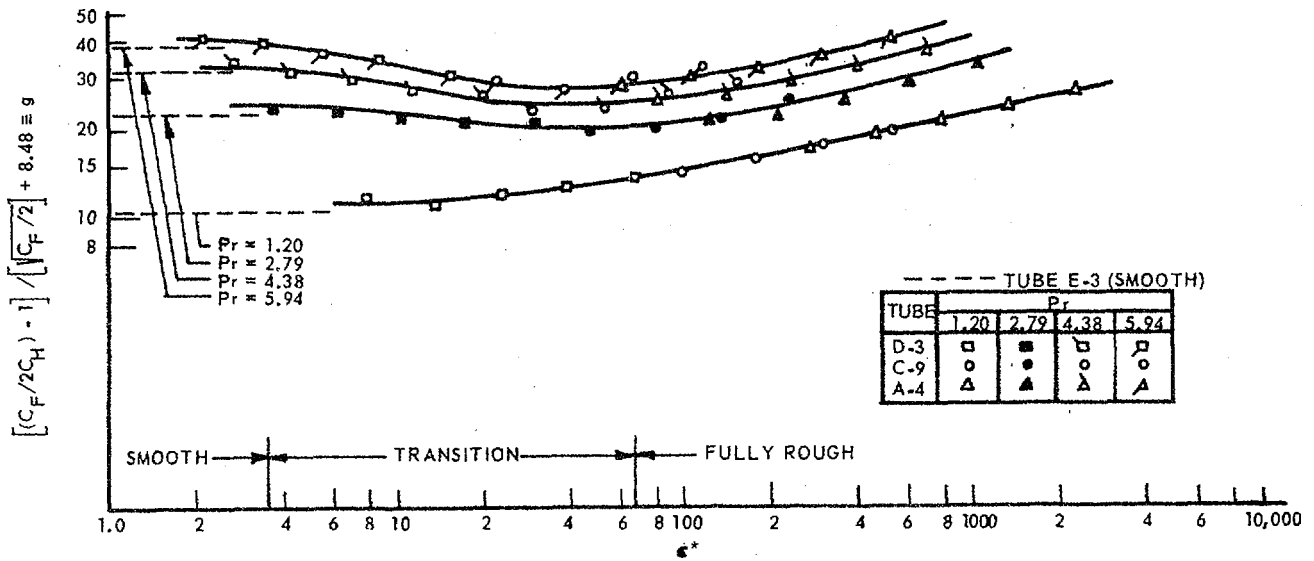


Fig. 7. Correlation of experimental results using the heat-transfer similarity law.

abscissa -  $K^*$   
 ordinate -  $g[K^*, Pr]$

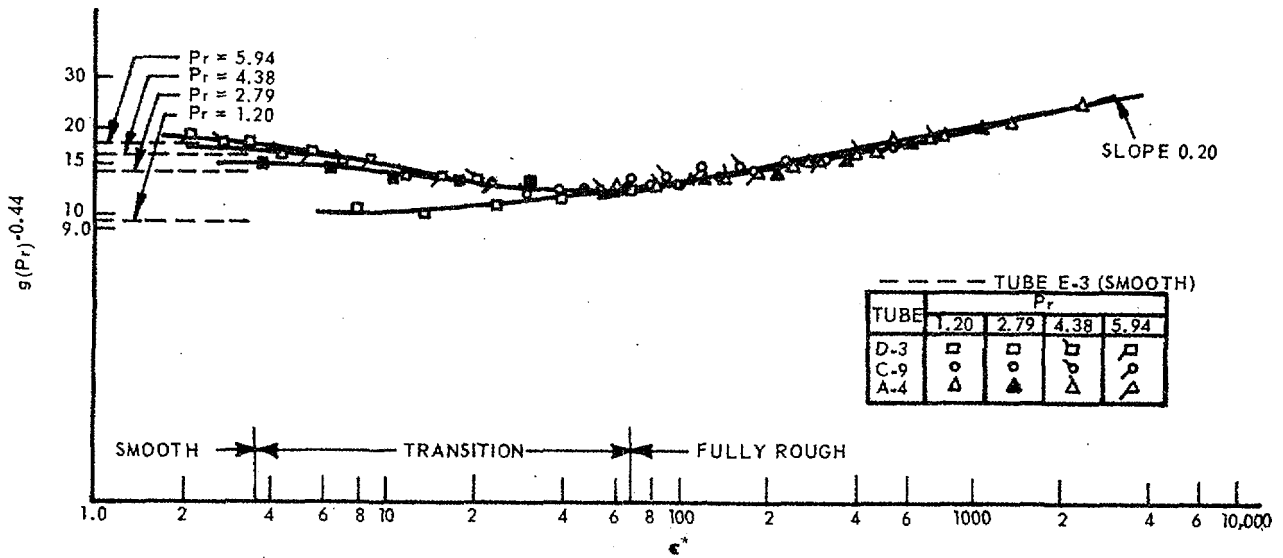


Fig. 8. Correlation of experimental results using the heat transfer similarity law and a power law for Prandtl number.

abscissa -  $K^*$   
 ordinate -  $g \cdot Pr^{-0.44}$

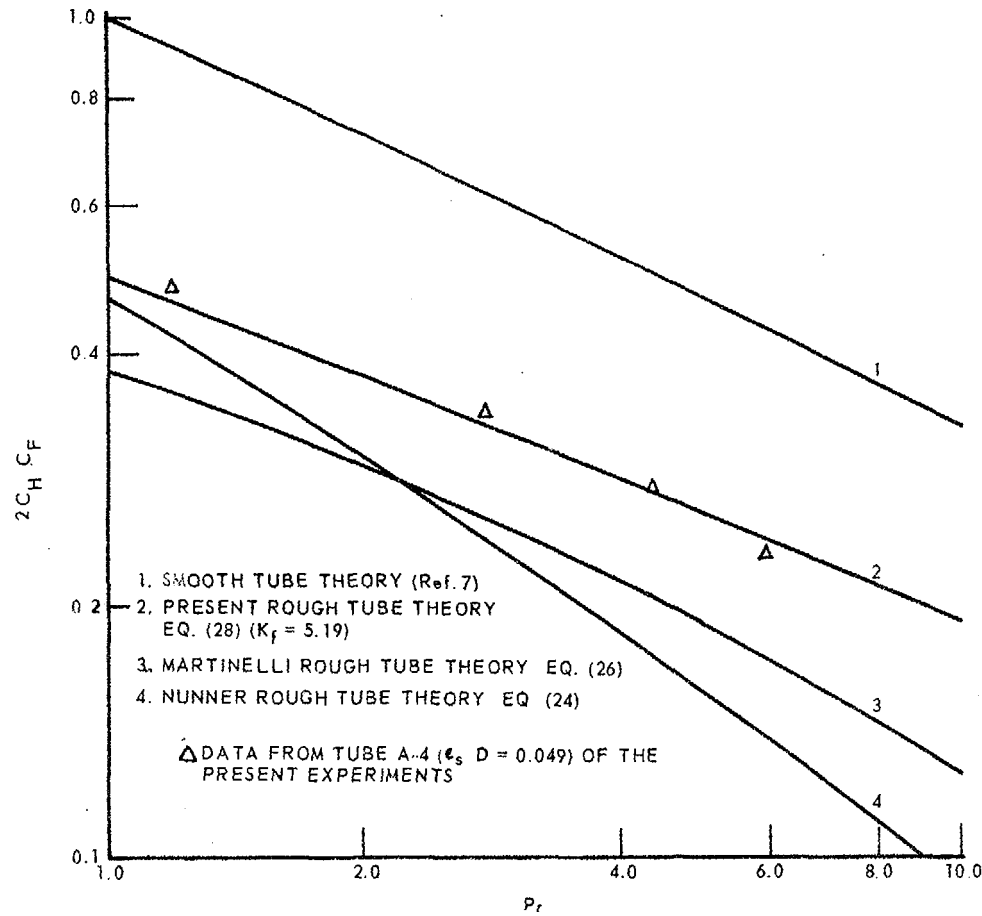
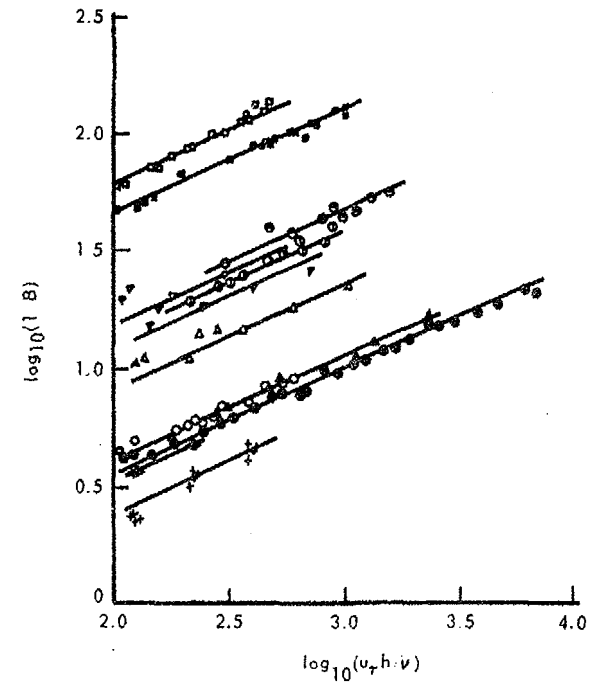


Fig. 9. Comparison of rough tube theories at  $Re = 1.5 \cdot 10^5$  and  $h/D = 0.049$  ( $f = 0.072$ ).  
 abscissa =  $Pr$   
 ordinate =  $8St/f$



Reference	Flow	Roughness type	$\sigma$
● Nunner	Pipe	Circumferential rings	0.72
○ Nunner	Pipe	Circumferential rings	0.72
◆ Pinkel	Pipe	Helical rings	0.72
+ Lancel	Channel	Pyramids	0.72
■ Cope	Pipe	Pyramids	7.3
□ Cope	Pipe	Pyramids	7.5
⊙ Owen, Thomson	Plate	Spanwise humps	3.2
⊙ Owen, Thomson	Plate	Irregular pyramids	3.2
▲ Dipprey	Pipe	Sand indentations	1.2
△ Dipprey	Pipe	Sand indentations	2.8
▼ Dipprey	Pipe	Sand indentations	4.4
▽ Dipprey	Pipe	Sand indentations	5.9

Fig. 10. The sublayer Stanton number: Reynolds number dependence.  
 abscissa -  $\log v_* h / \nu$   
 ordinate -  $\log 1/St_{sub}$   
 $\sigma = Pr$ .

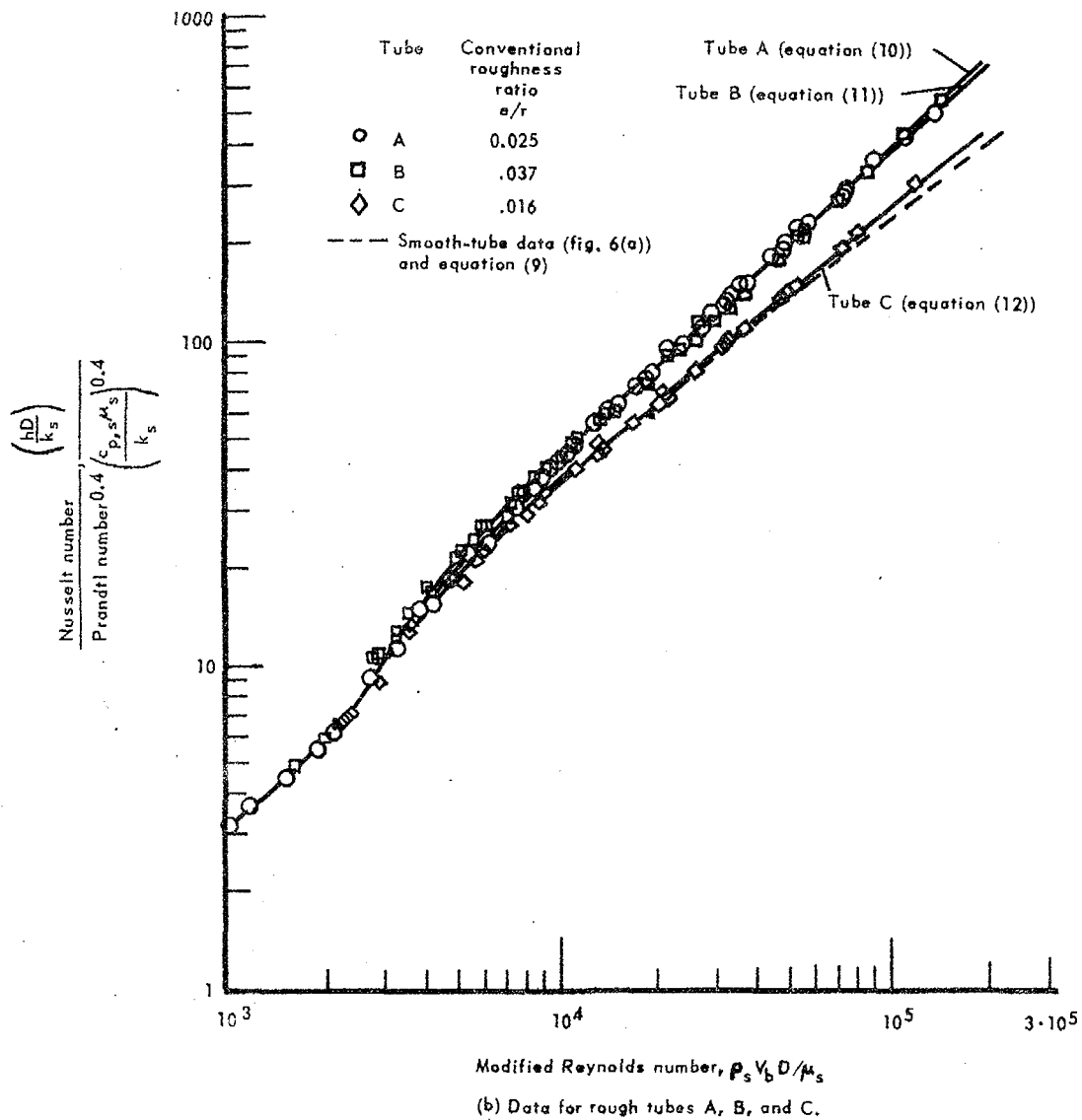


Fig. 11. Correlation of heat transfer data with modified surface Reynolds number. Physical properties of air evaluated at average surface temperature  $T_s$ .

abscissa -  $\rho_s v_b D / \mu_s$   
 ordinate -  $Nu / Pr^{0.4}$

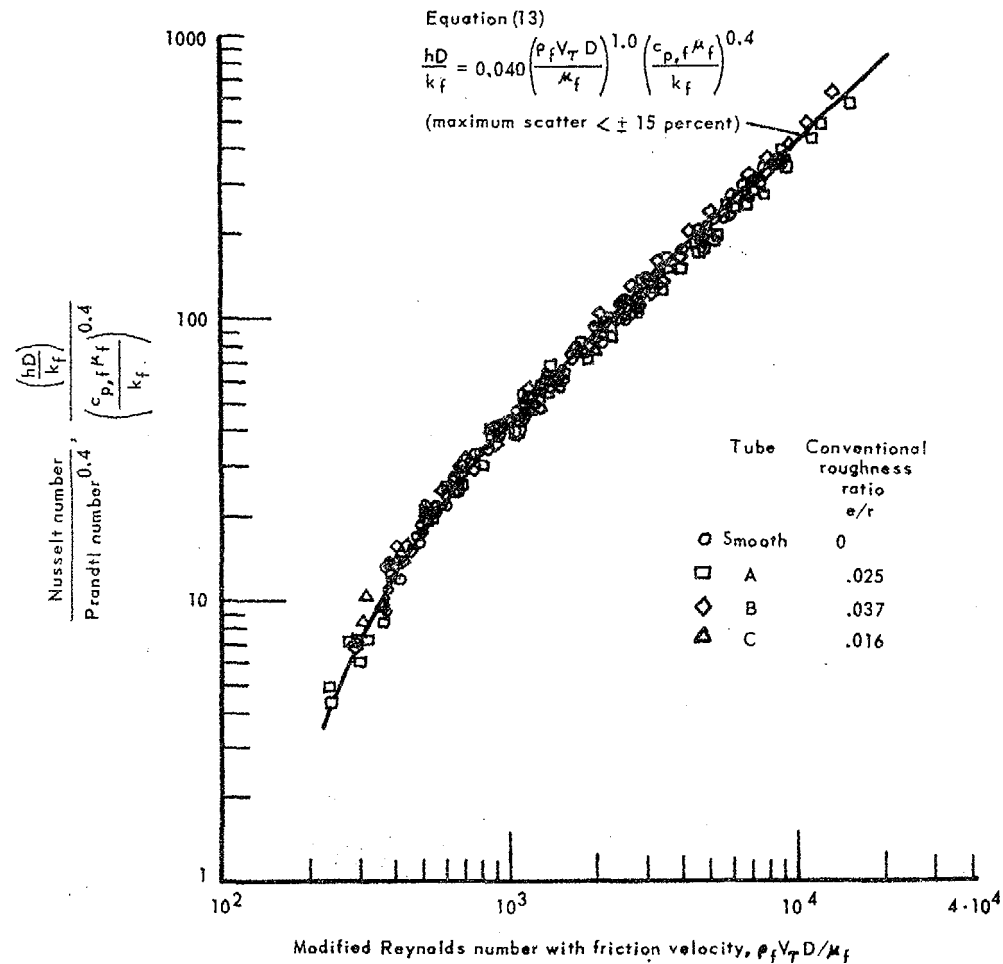


Fig. 12. Correlation of heat transfer data with modified film Reynolds number and friction velocity. Physical properties of air evaluated at average film temperature  $T_f$ .

abscissa -  $\rho_{\text{film}} v_* D / \mu_{\text{film}}$   
 ordinate -  $Nu / Pr^{0.4}$

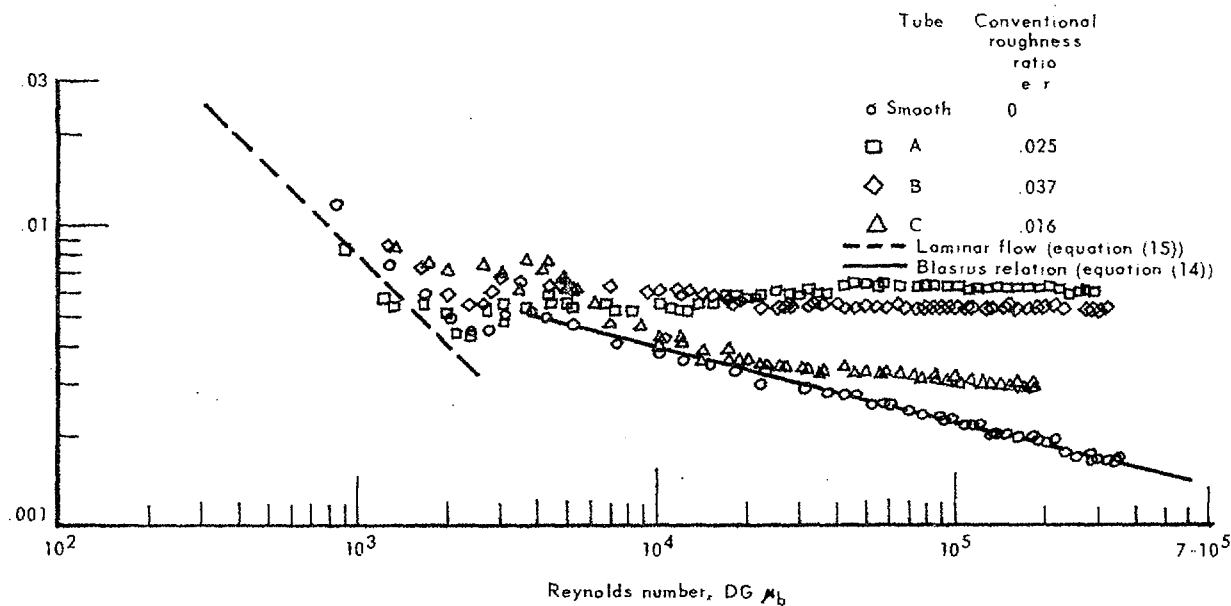


Fig. 13. Comparison of isothermal friction coefficients for smooth tube and the rough tubes.

abscissa -  $Re$

ordinate -  $f/8$

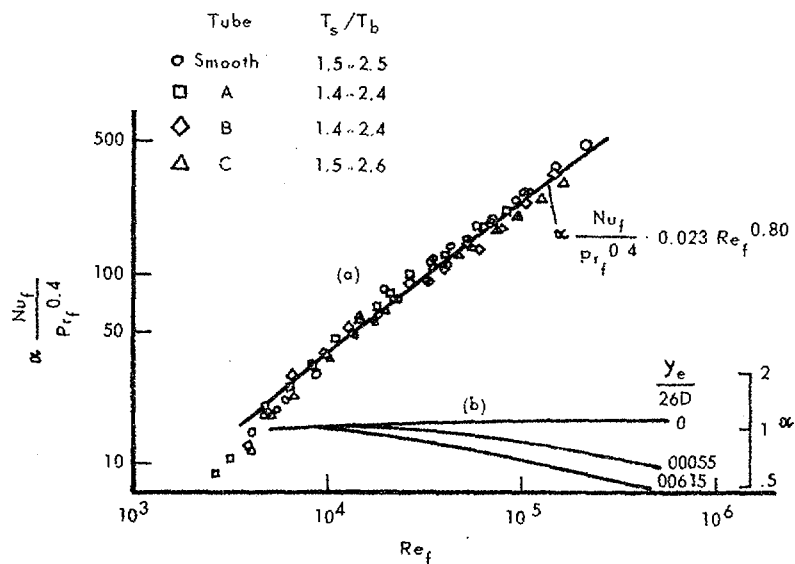


Fig. 14. Correlation of heat transfer data for various roughness for a range of  $T_s/T_b$  from 1.4 to 2.5.

abscissa -  $Re_{film}$  for (a)

ordinate -  $A \cdot Nu/Pr^{0.4}$

abscissa -  $Re_{film}$  for (b)

ordinate -  $A$

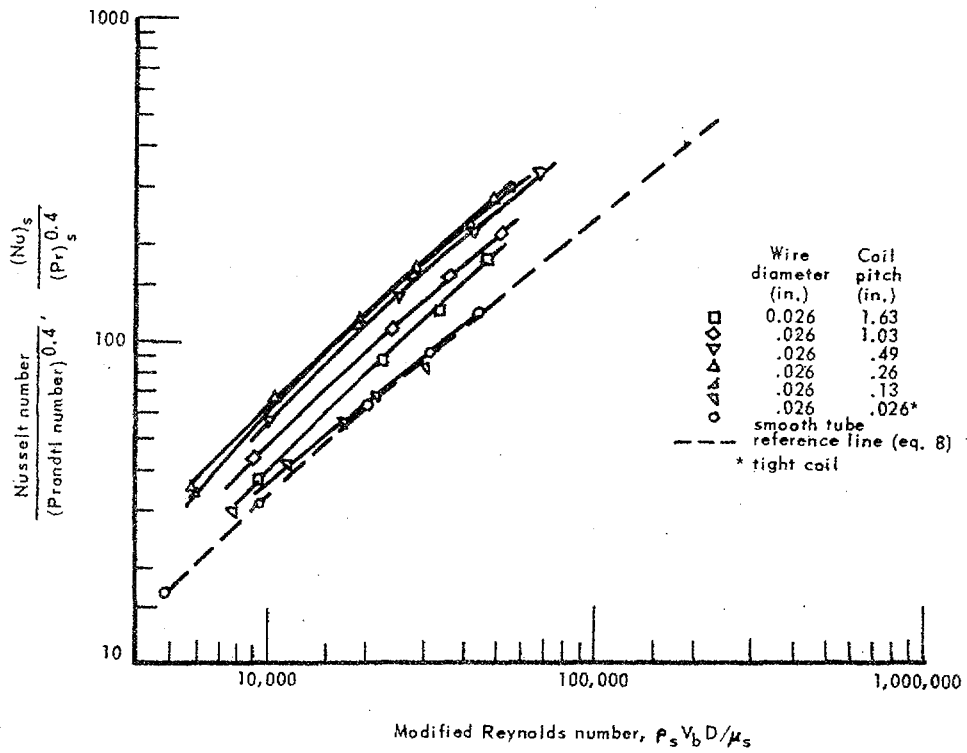


Fig. 15. Heat transfer data for all wire coils of 0.66 mm diameter wire.

abscissa -  $Re_{mod}$

ordinate -  $Nu_s / Pr_s^{0.4}$

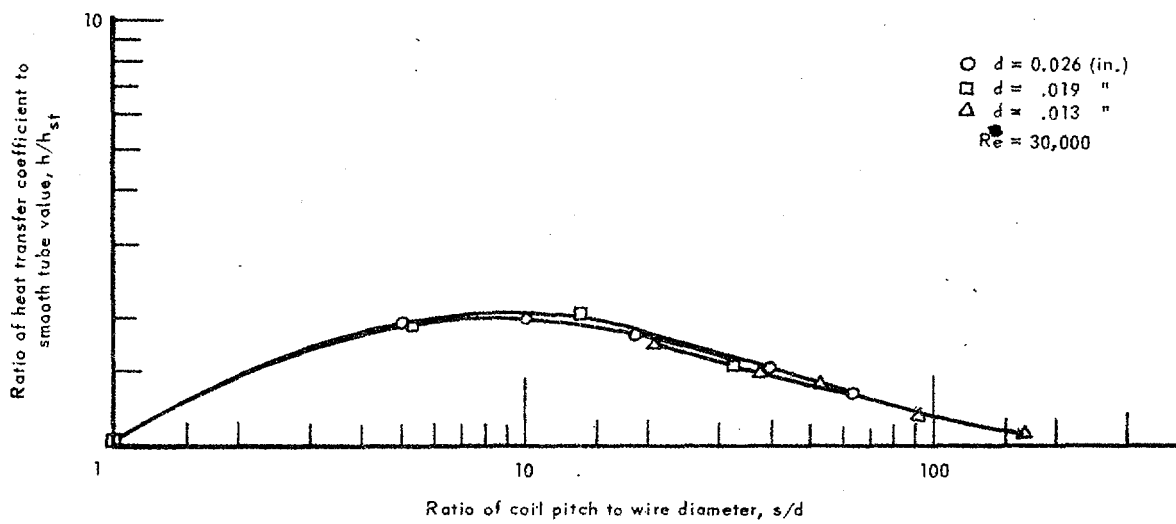


Fig. 16. Variation of  $\alpha/\alpha_0$  with  $p/k$ .

abscissa -  $p/k$

ordinate -  $\alpha/\alpha_0$

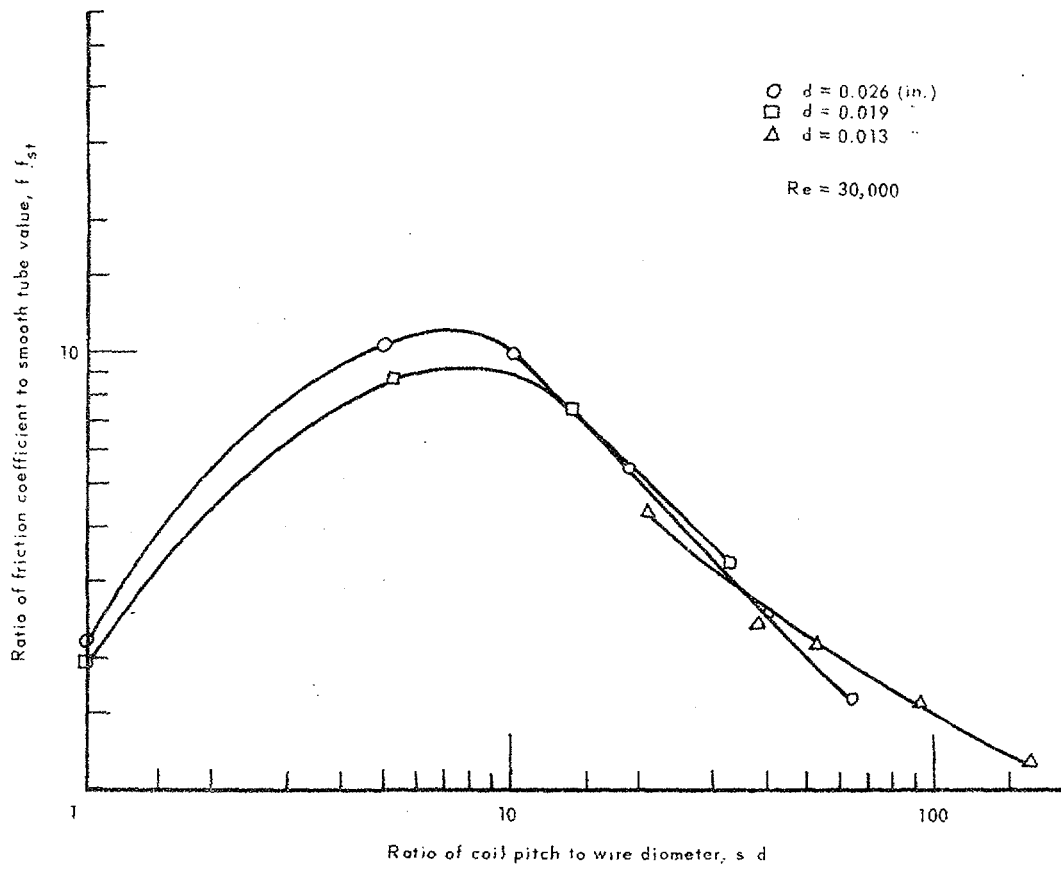


Fig. 17. Variation of  $f/f_0$  with  $p/k$ .

abscissa -  $p/k$

ordinate -  $f/f_0$

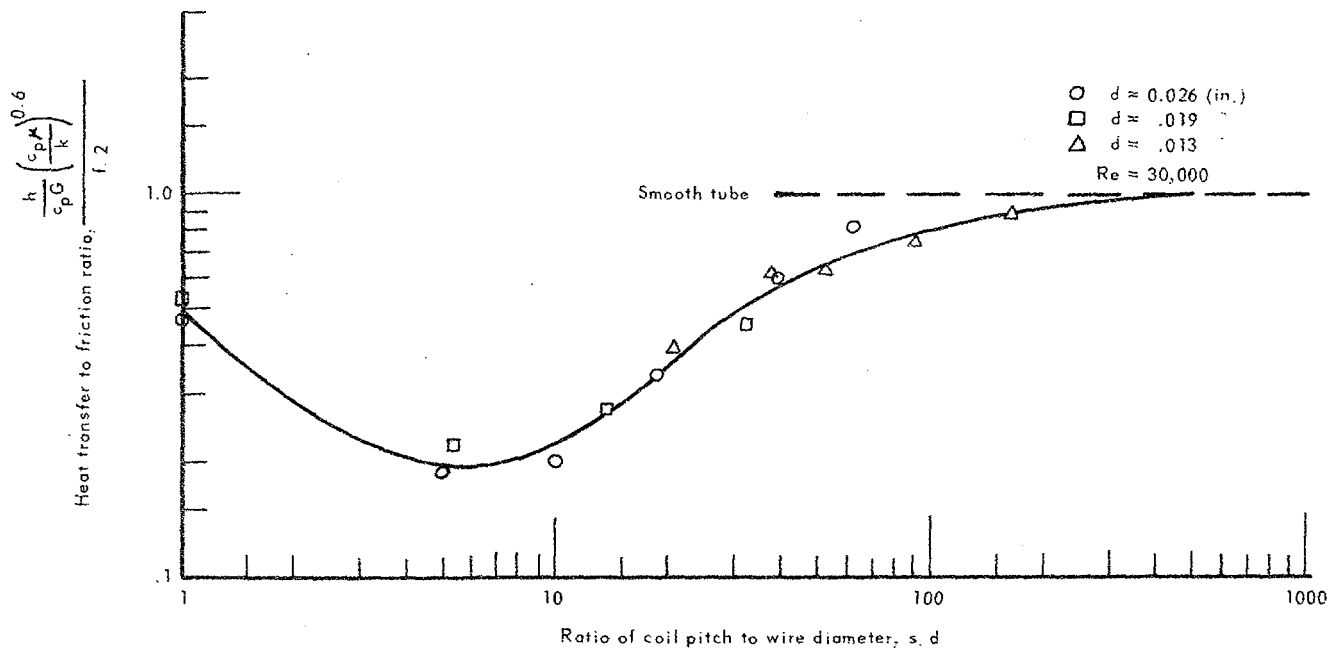


Fig. 18. Variation of heat transfer to friction ratio with  $p/k$ .

abscissa -  $p/k$

ordinate -  $\frac{Nu \cdot Pr^{0.6}}{f}$

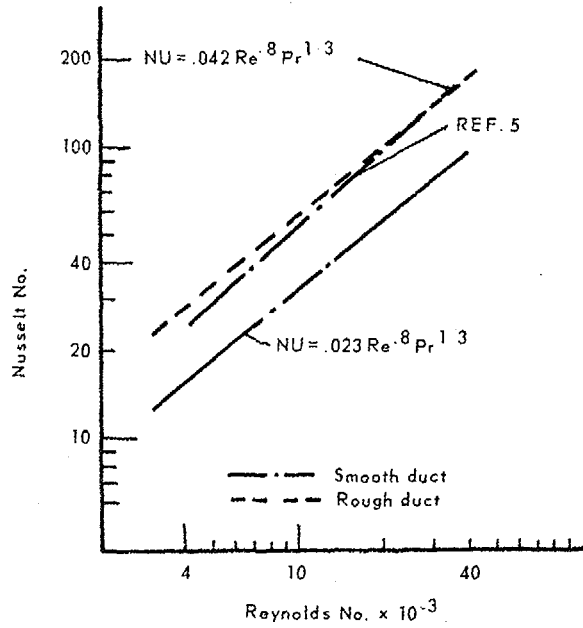


Fig. 19. Comparison of smooth and rough-duct results.

abscissa -  $Re$

ordinate -  $Nu$  (REF. 5 indicates ref. 28 in this literature survey)

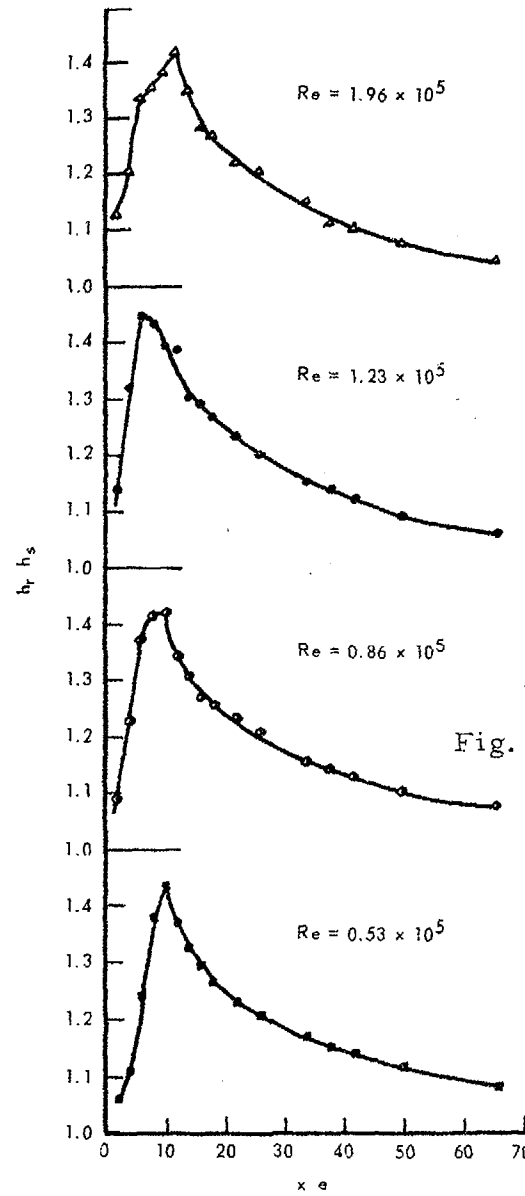


Fig. 20. The effect of Reynolds number on the improvement in the local heat transfer coefficient produced by a wire 1.59 mm in diameter.

abscissa -  $x/k$  where  $x$  = distance measured downstream from roughness wire under consideration.

ordinate -  $\frac{h_r}{h_s}$

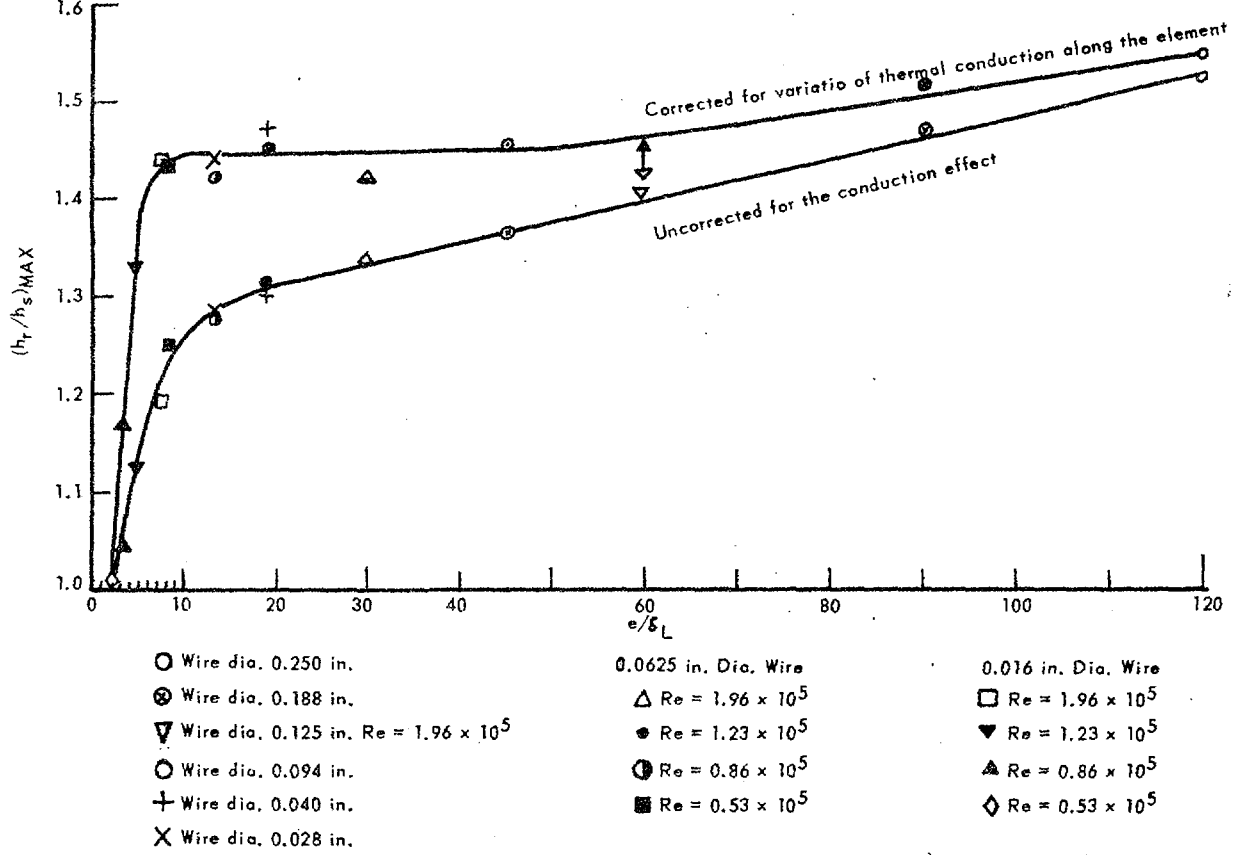


Fig. 21. The effect of Reynolds number and wire size on  $(\alpha/\alpha_0)_{max}$ .

abscissa -  $k/\delta_L$

ordinate -  $(\alpha/\alpha_0)_{max}$ .

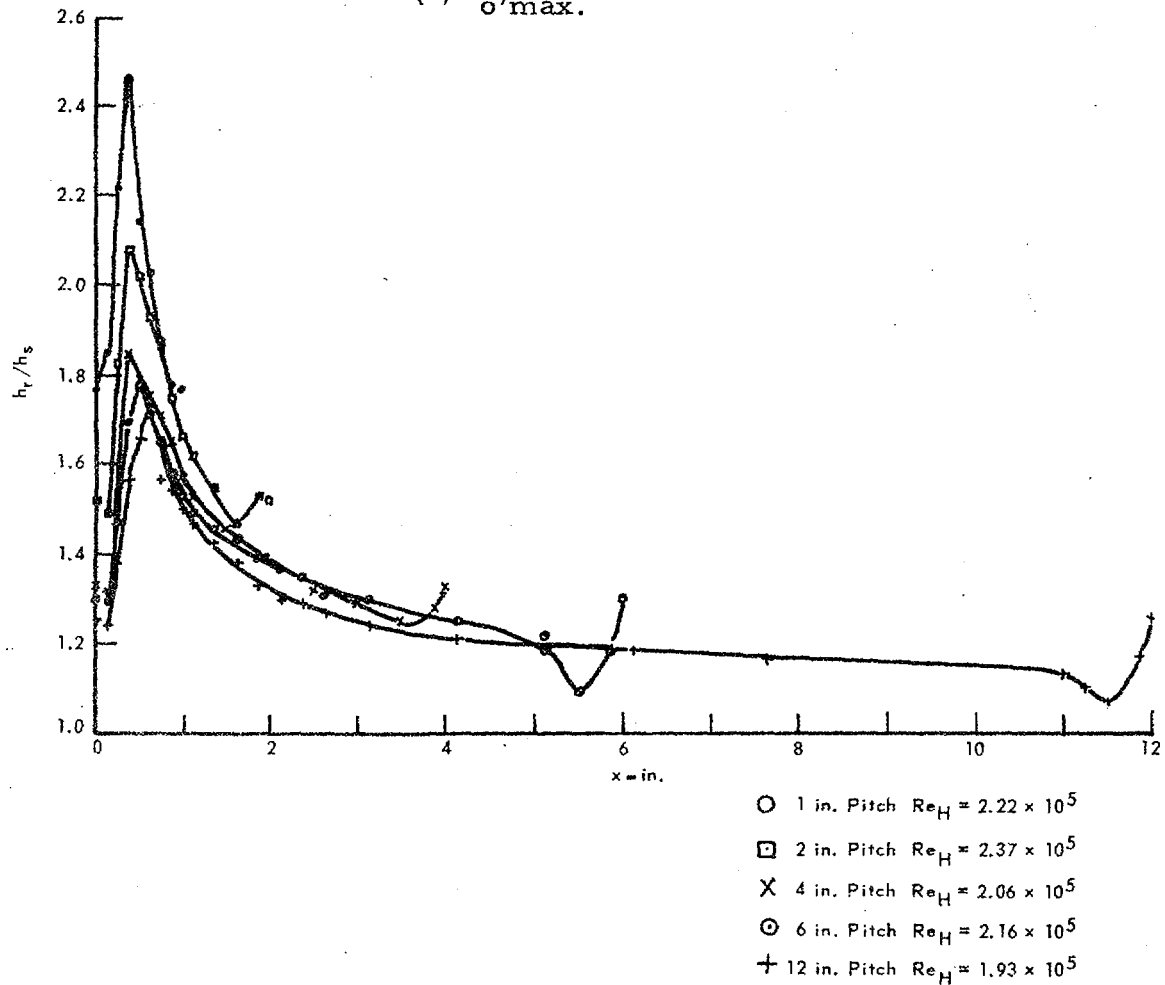


Fig. 22. Multiple wire tests: the variation of  $\alpha/\alpha_0$  between wires at various pitches.

abscissa -  $x$  (see fig. 20)

ordinate -  $\alpha/\alpha_0$

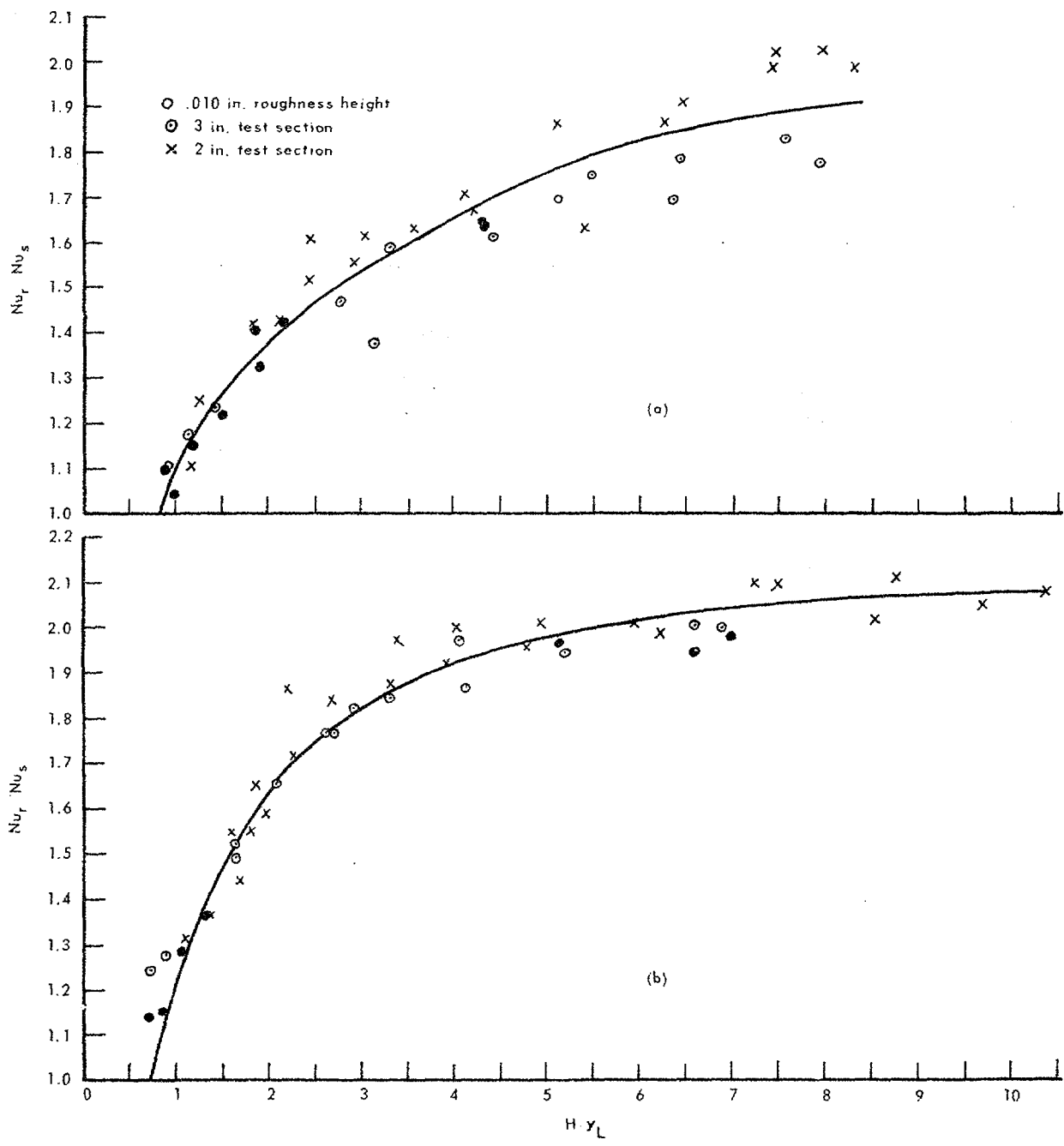


Fig. 23. Variation of  $Nu_r/Nu_o$  with  $k/\delta_L$ : (a)  $p/k = 5.0$   
 (b)  $p/k = 10.0$

abscissa -  $Nu_r/Nu_o$

ordinate -  $k/\delta_L$

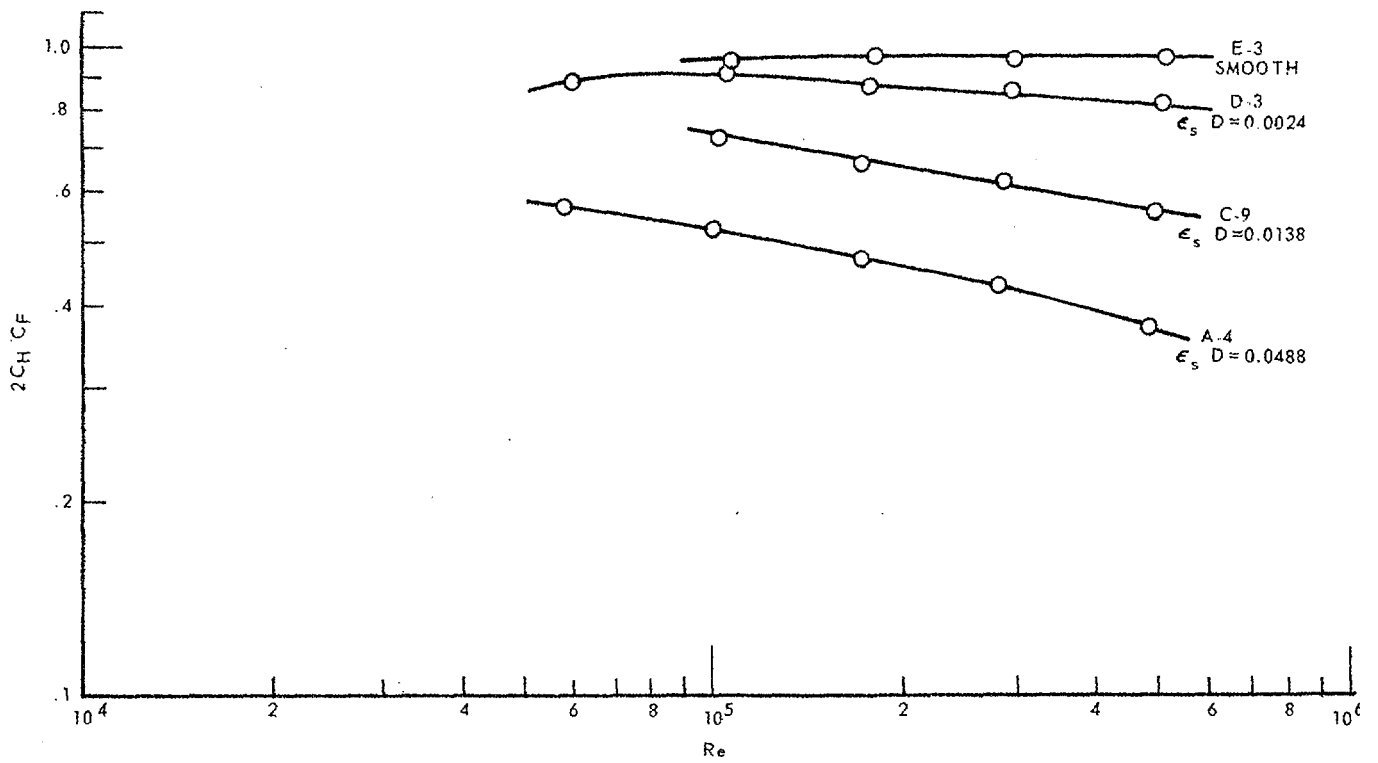


Fig. 24. Comparison of heat-transfer and friction coefficients vs Reynolds number for Pr. = 1.20.

abscissa - Re

ordinate -  $8St/f$

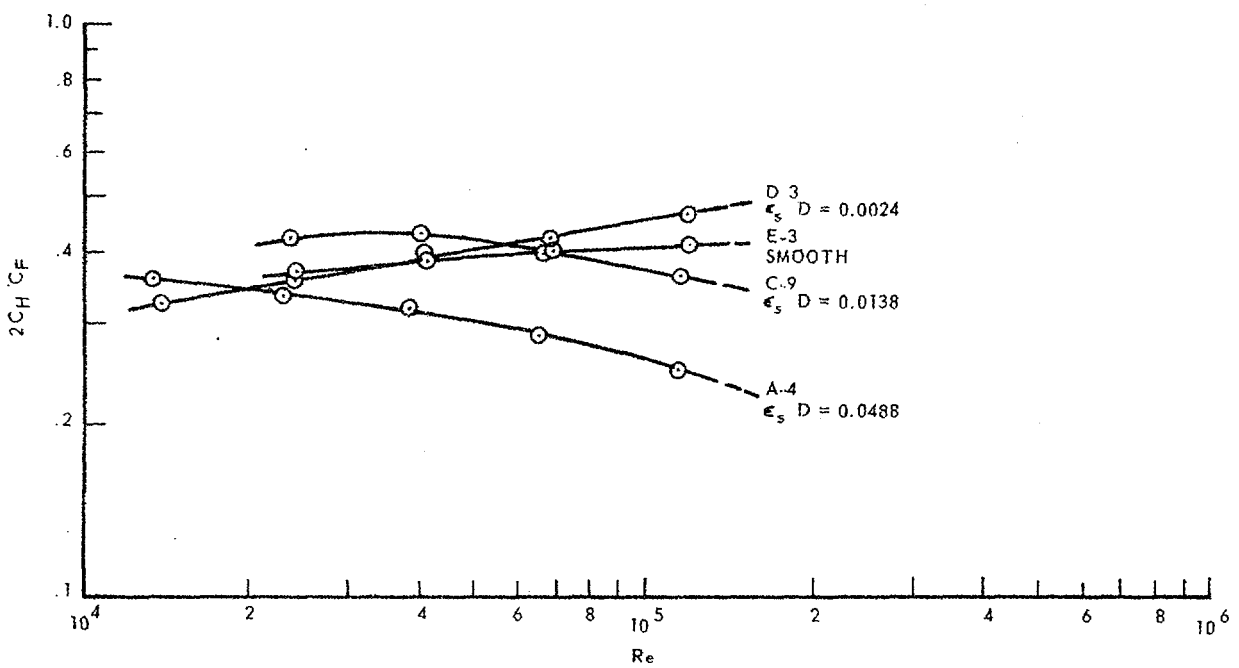


Fig. 25. Comparison of heat-transfer and friction coefficients vs Reynolds number for Pr. = 5.94.

abscissa - Re

ordinate -  $8St/f$

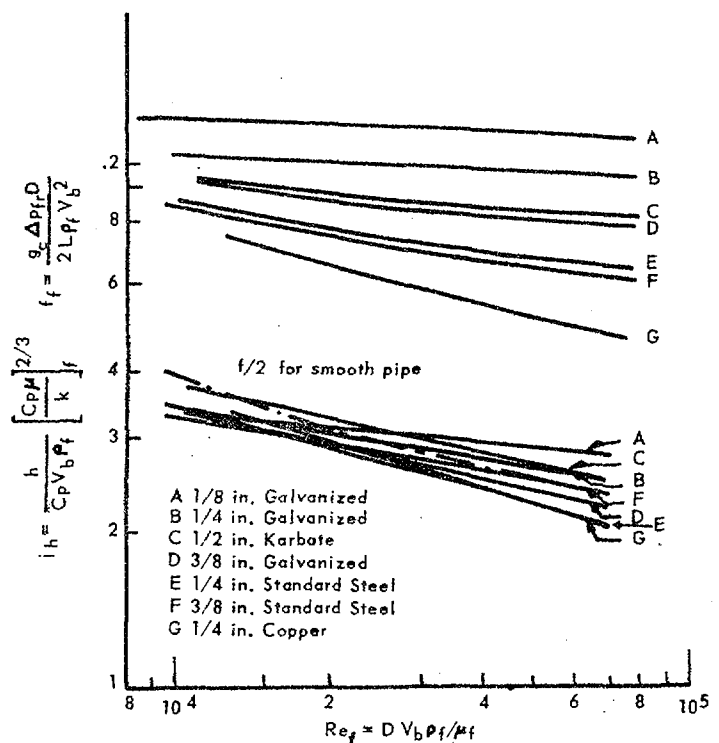


Fig. 26. Fluid friction and heat transfer curves for seven commercial pipes.

abscissa -  $Re_f$   
 ordinate -  $St. Pr^{2/3}$  and  $f_f/4$

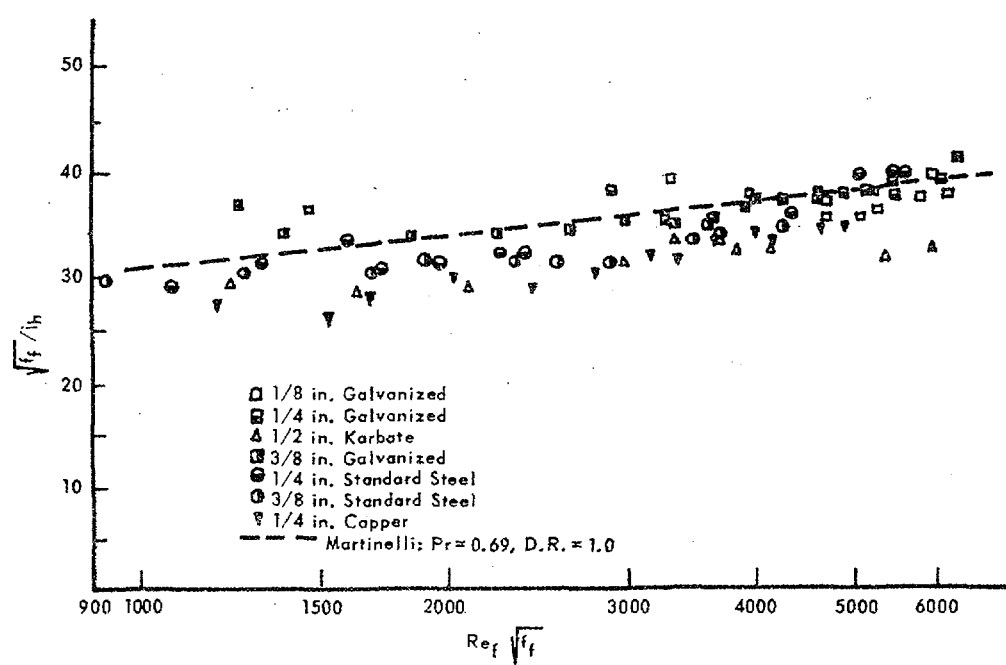


Fig. 27. Test of Martinelli's analogy

abscissa -  $\log Re_f \sqrt{f_f/4}$   
 ordinate -  $\log \sqrt{f_f/4} St. Pr^{2/3}$

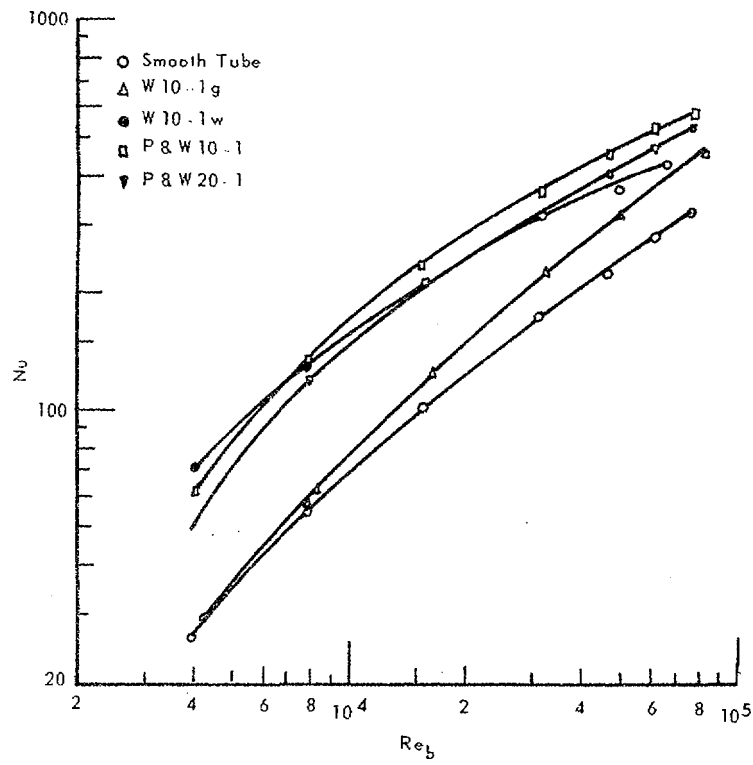


Fig. 28. Nusselt number vs Reynolds number for different roughness.

abscissa -  $Re$

ordinate -  $Nu$

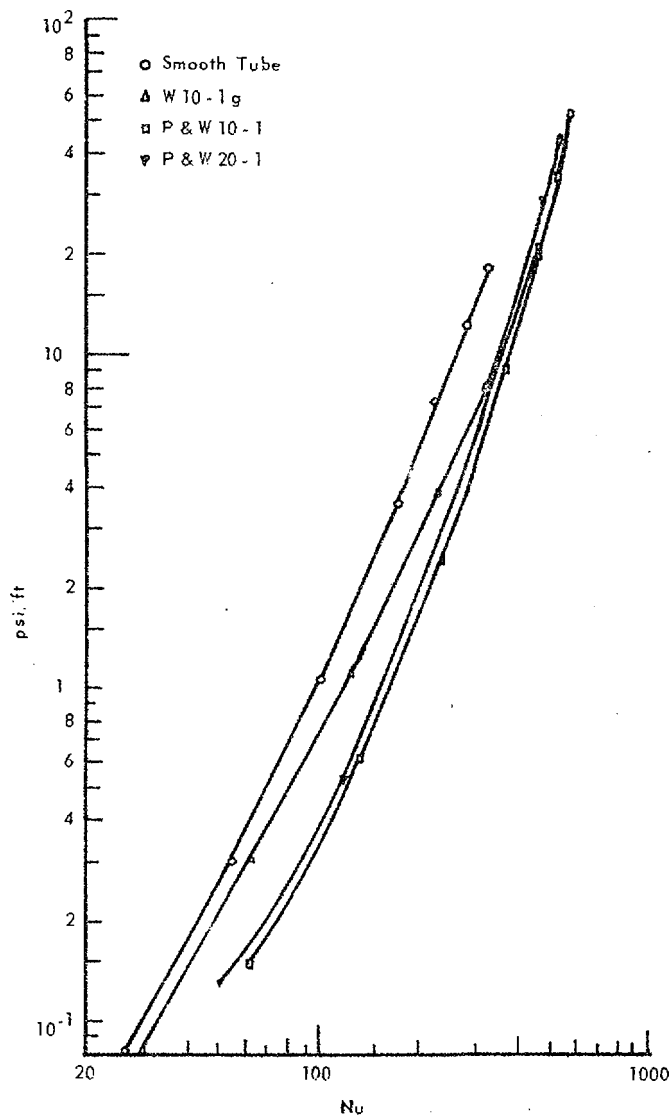


Fig. 29. Pressure drop per unit length vs Nusselt number.

abscissa -  $Nu$

ordinate - pounds per square inch/foot

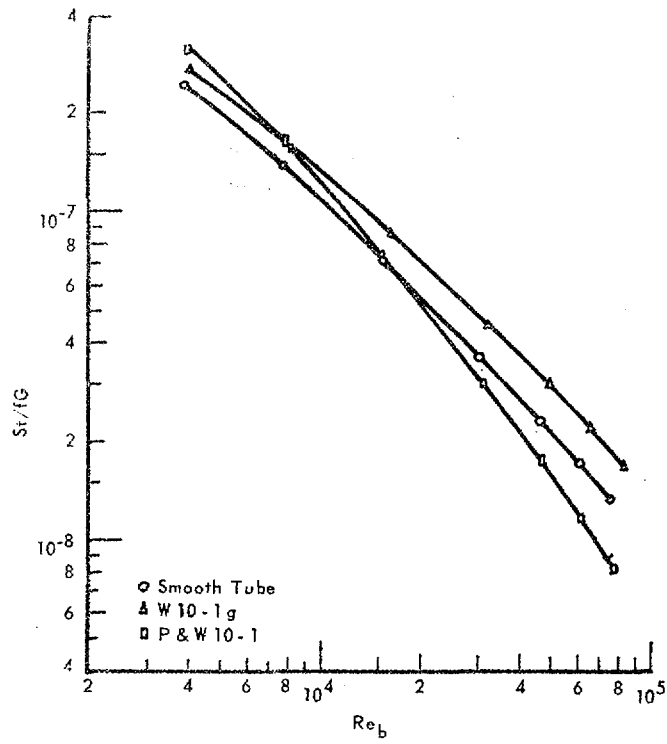


Fig. 30. Heat transfer to pressure drop ratio vs bulk Reynolds number.

abscissa -  $Re$

ordinate -  $4St/fG$

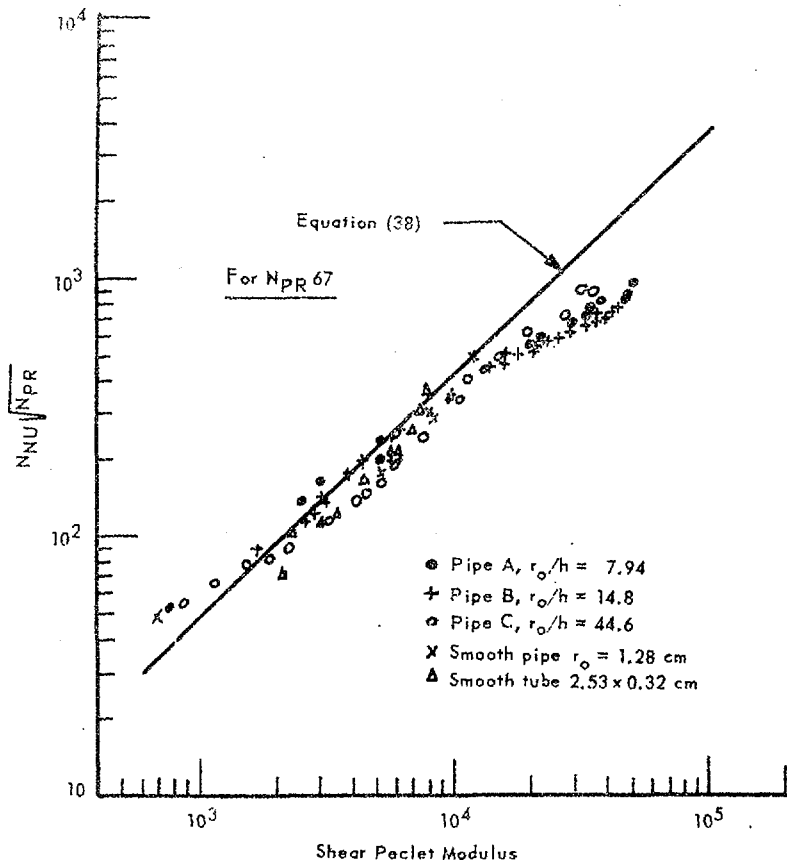


Fig. 31. Test of equation, suggested by Martinelli (24) for data from experiment of Cope (4).

abscissa -  $Re \cdot Pr \cdot f/8$

ordinate -  $Nu \cdot \sqrt{Pr}$

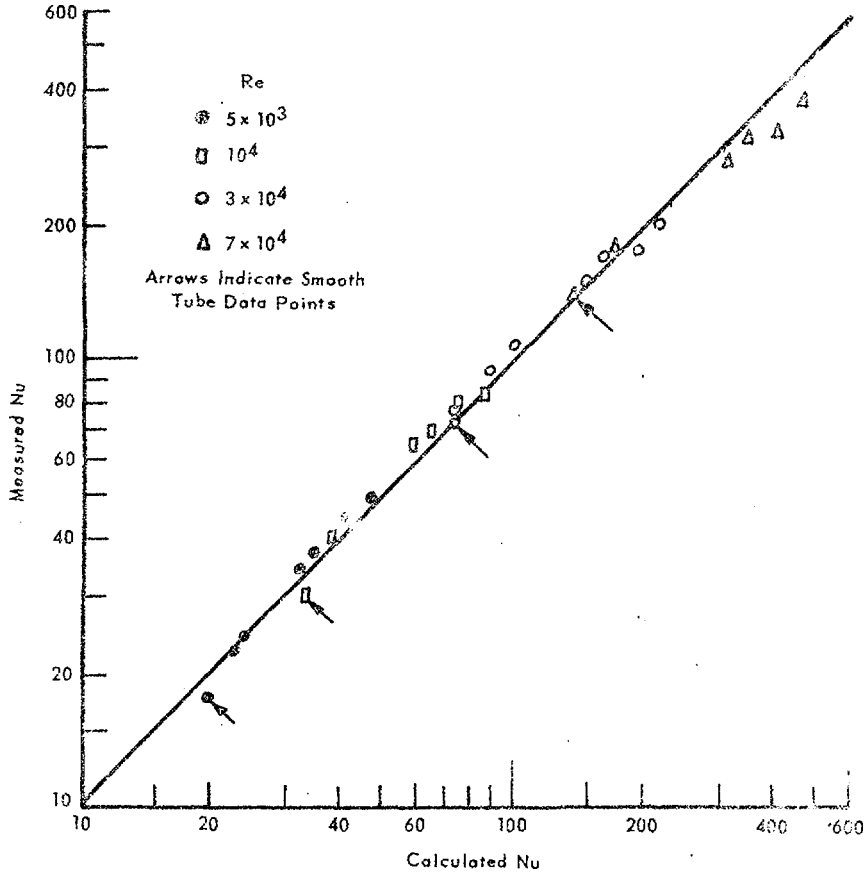


Fig. 32. Test of Martinelli's equation with Nunner's (28) data.

abscissa - Calculated Nu

ordinate - Measured Nu

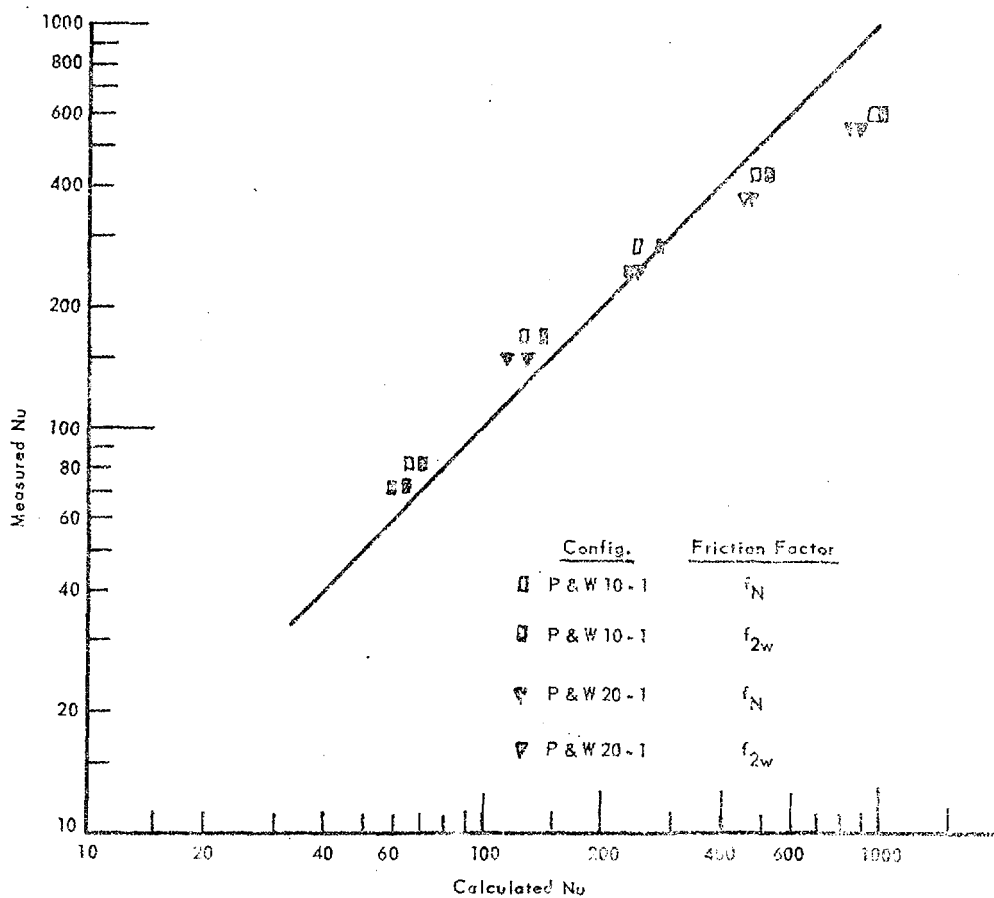


Fig. 33. Test of Martinelli's equation with data from experiment by Kemeny & Cyphers (20).

abscissa - Calculated Nu

ordinate - Measured Nu

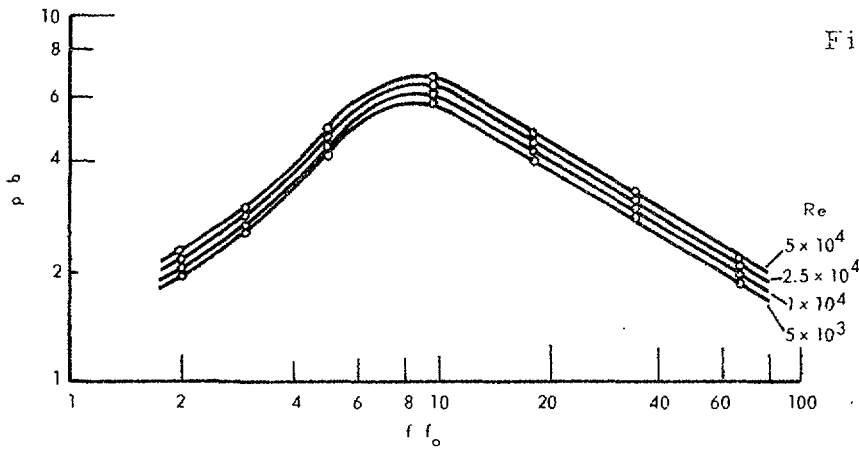


Fig. 34. Corrected friction factor  $f/f_0$  dependent on the spacing ratio  $p/b$  and the Reynolds number  $Re$  for a narrow annulus, when  $d_o/d_i = 1.287$ .  
abscissa -  $f/f_0$   
ordinate -  $p/b$

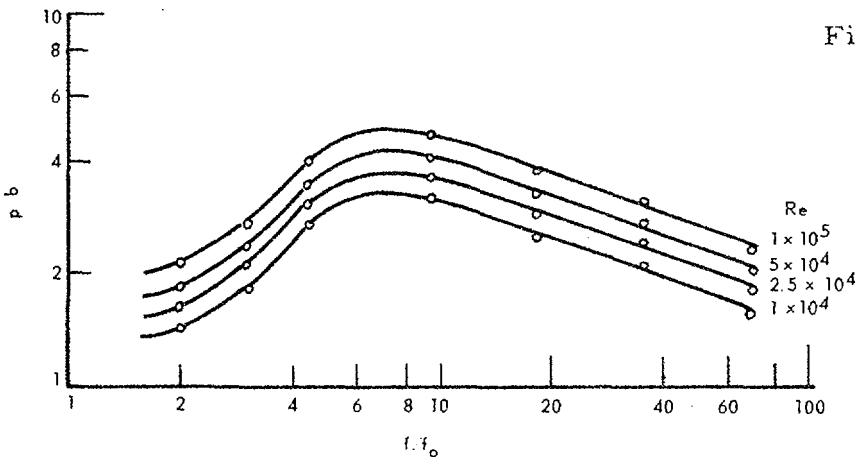


Fig. 35. Corrected friction factor  $f/f_0$  dependent on the spacing ratio  $p/b$  and the Reynolds number  $Re$  for a wide annulus when  $d_o/d_i = 1.728$ .  
abscissa -  $f/f_0$   
ordinate -  $p/b$

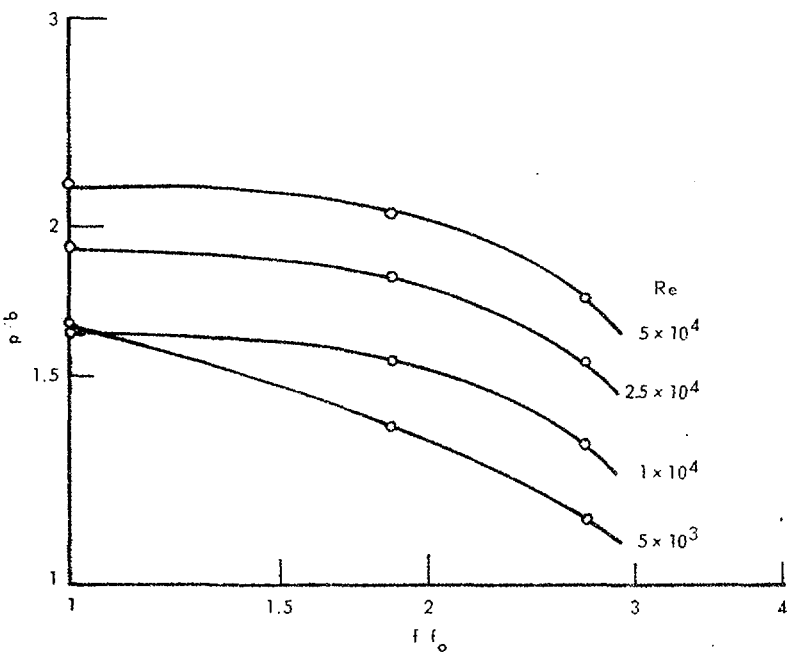


Fig. 36. Corrected friction factor  $f/f_0$  dependent on the spacing ratio  $p/b$  and the Reynolds number  $Re$  for a narrow annulus when  $d_o/d_i = 1.287$ .  
abscissa -  $f/f_0$   
ordinate -  $p/b$

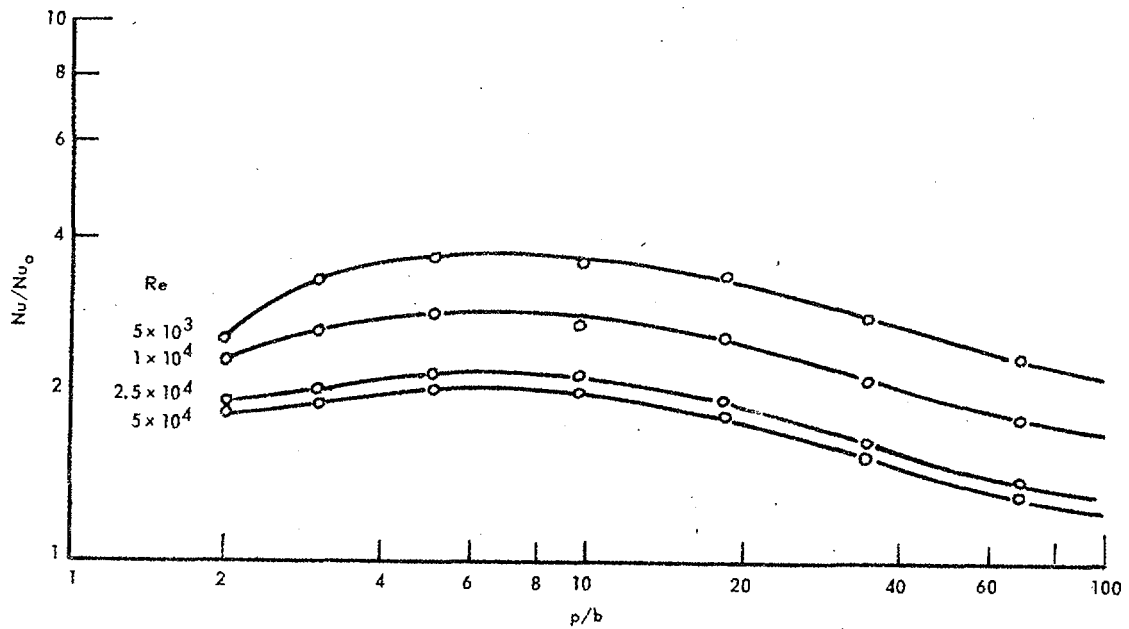


Fig. 37. Corrected Nusselts number  $Nu/Nu_0$ , dependent on the spacing ratio  $p/b$  and the Reynolds number  $Re$  for a narrow annulus when  $d_o/d_i = 1.287$ .

abscissa -  $p/b$   
 ordinate -  $Nu/Nu_0$

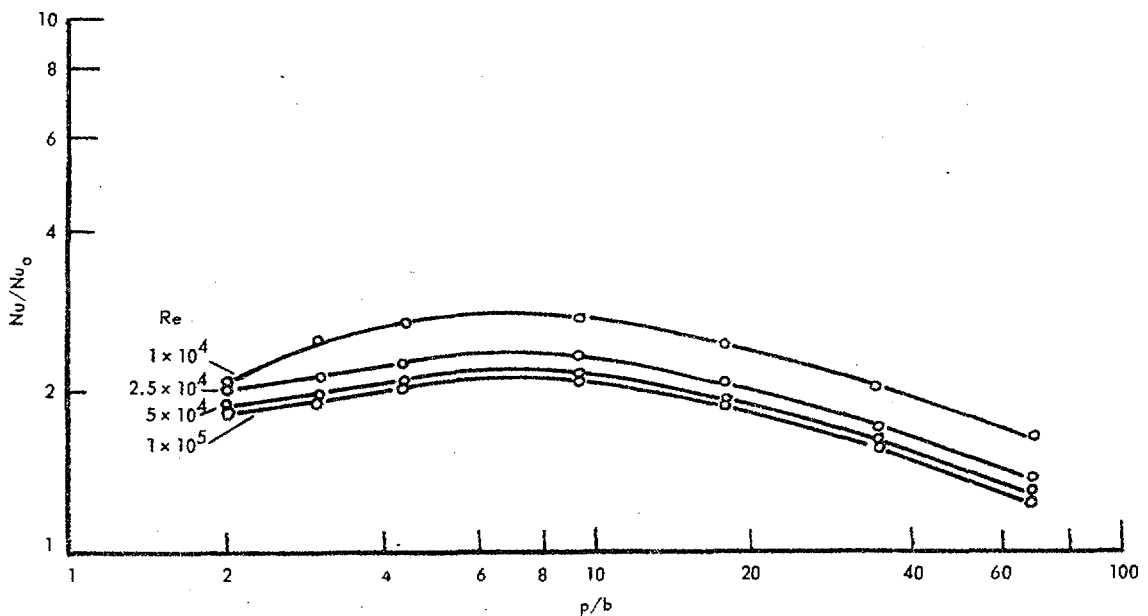


Fig. 38. Corrected Nusselts number  $Nu/Nu_0$ , dependent on the spacing ratio  $p/b$  and the Reynolds number  $Re$  for a wide annulus, when  $d_o/d_i = 1.728$ .

abscissa -  $p/b$   
 ordinate -  $Nu/Nu_0$

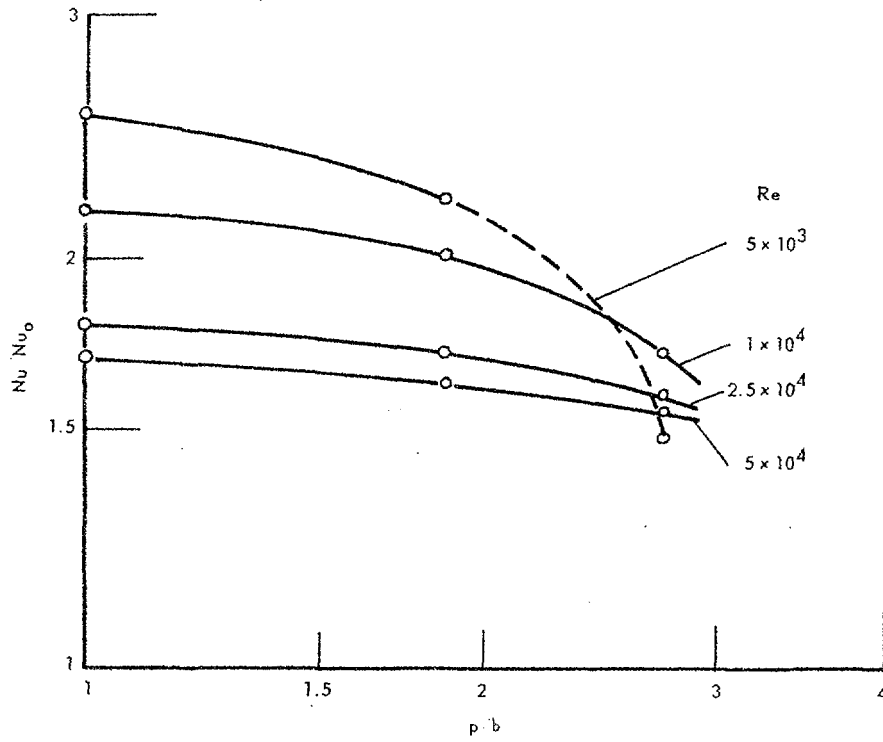


Fig. 39. Corrected Nusselts number  $Nu/Nu_0$ , dependent on the spacing ratio  $p/b$  and the Reynolds number  $Re$  for a narrow annulus, when  $d_o/d_i = 1.287$ .

abscissa -  $p/b$

ordinate -  $Nu/Nu_0$

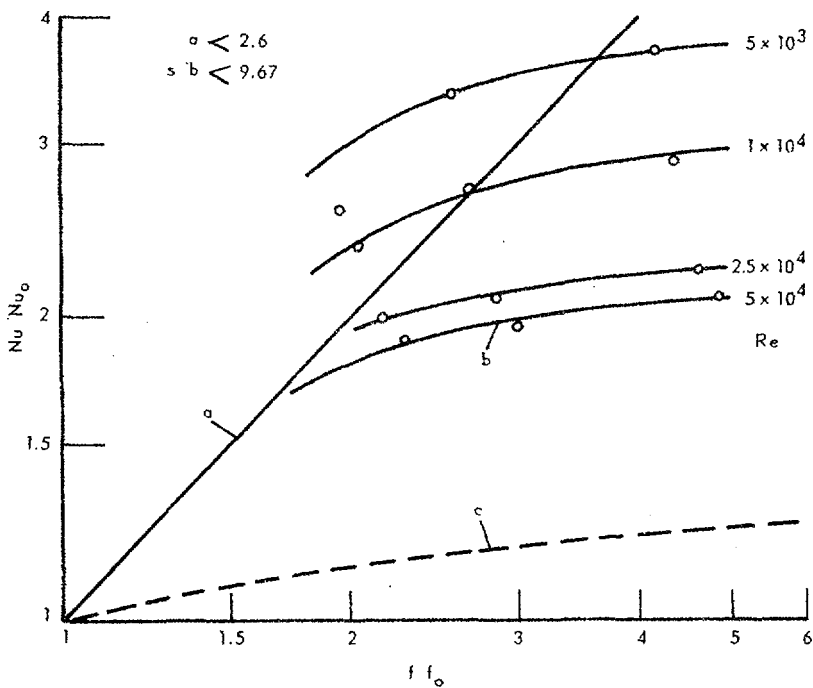


Fig. 40. Corrected Nusselt number  $Nu/Nu_0$  dependent on the corrected friction factor  $f/f_0$  for a narrow annulus when  $d_o/d_i = 1.287$ .

$p-b < 2.6$  mm

abscissa -  $f/f_0$

ordinate -  $Nu/Nu_0$

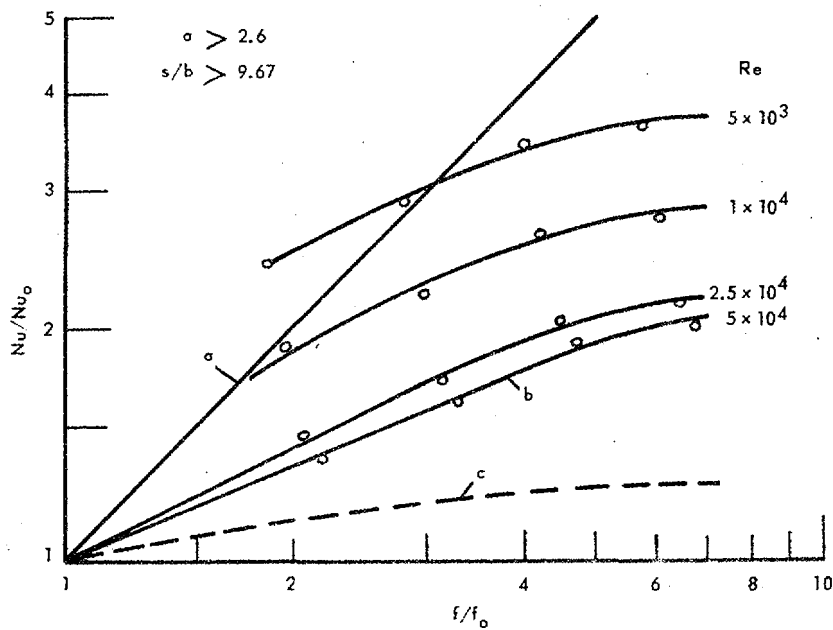


Fig. 41. Corrected Nusselt number  $Nu/Nu_0$  dependent on the corrected friction factor  $f/f_0$  for a narrow annulus when  $d_0/d_1 = 1.287$ .  
 $p-b > 2.6$  mm  
 abscissa -  $f/f_0$   
 ordinate -  $Nu/Nu_0$

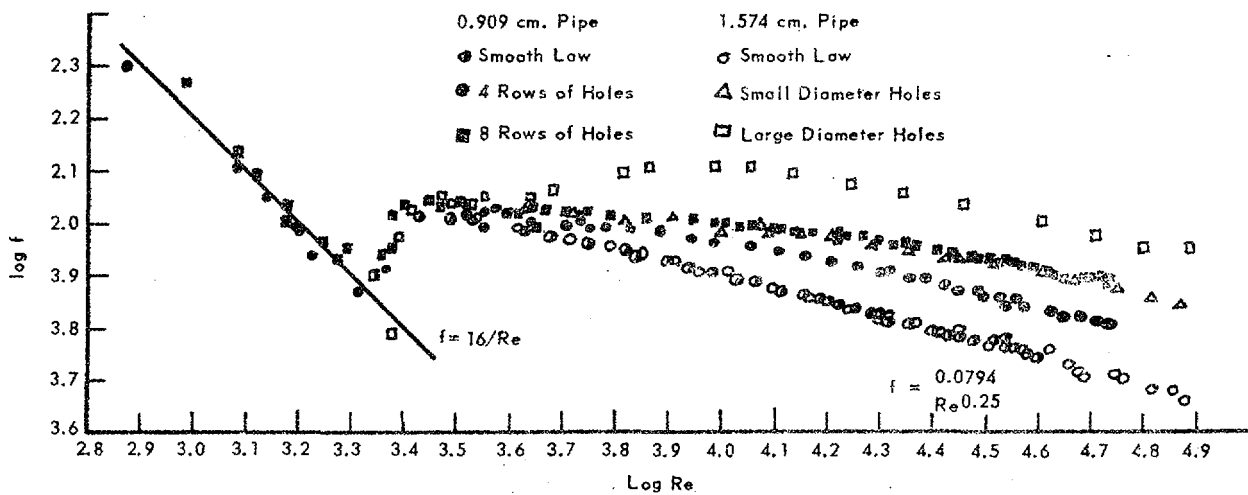


Fig. 42. Friction coefficients for pipes having artificially roughened surfaces plotted against Reynolds number. Nature of roughness elements - drilled holes.  
 abscissa -  $\log Re$   
 ordinate -  $\log f$

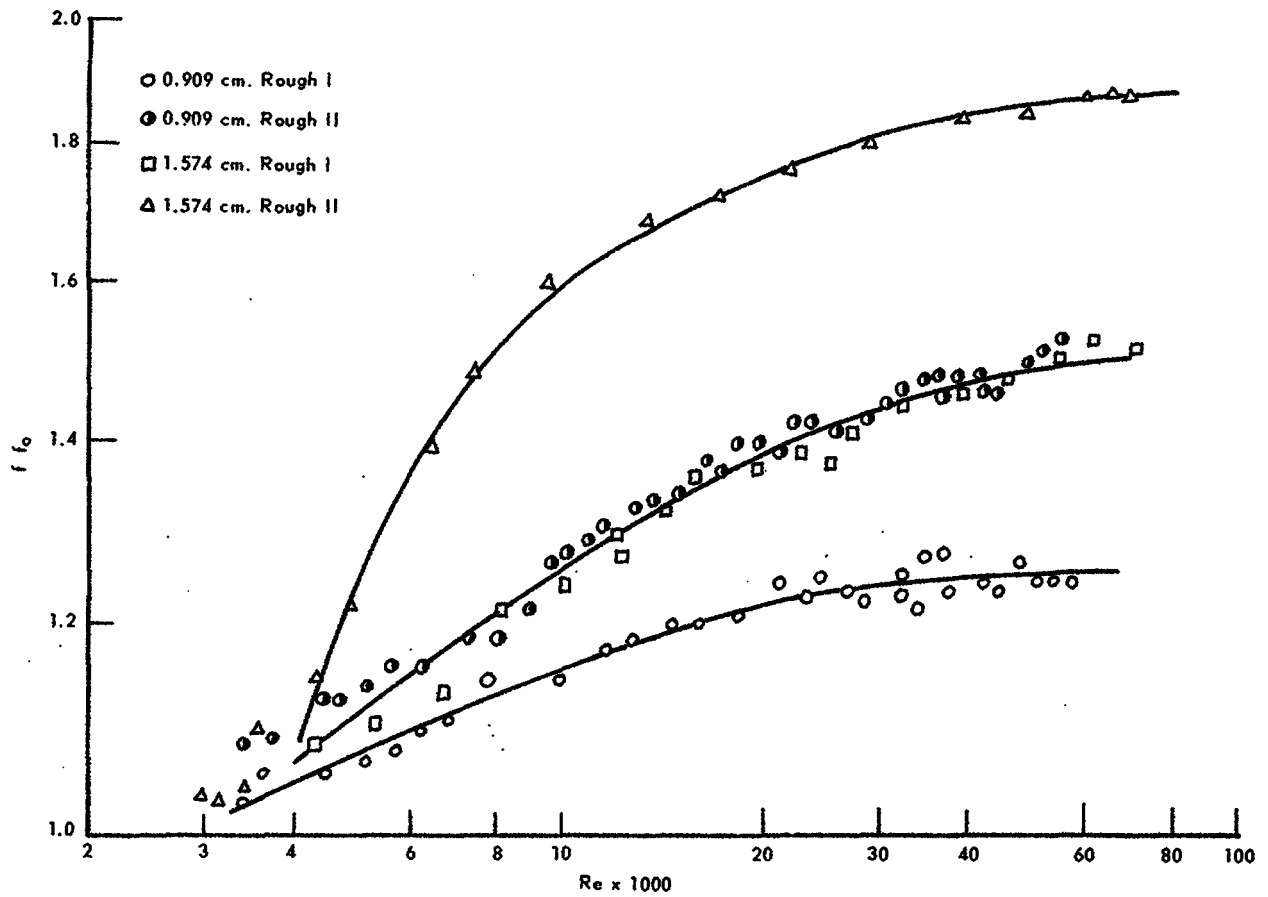


Fig. 43. Corrected friction factor plotted against Reynolds number.  
 abscissa -  $Re \times 1000$   
 ordinate -  $f/f_0$

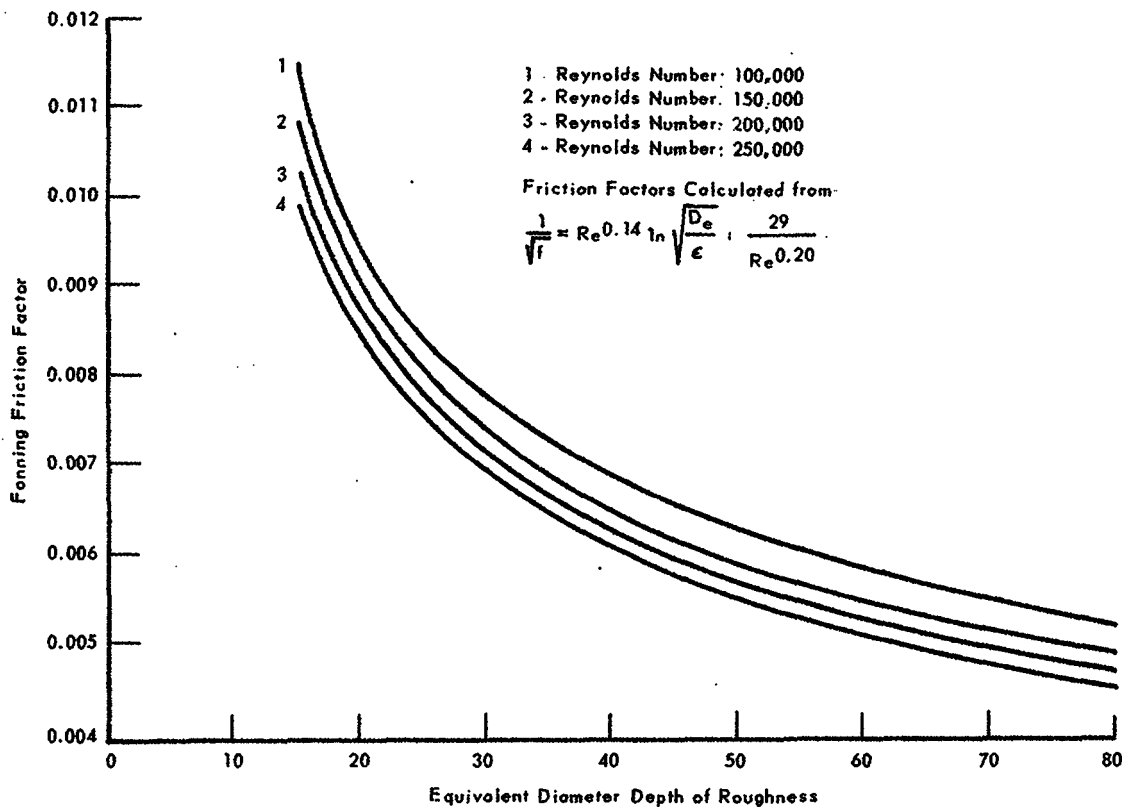


Fig. 44. Calculated friction factors for an annulus with  
 $d_i = 12.7$  mm with 36% of wetted perimeter roughened  
 with medium diamond knurls.  
 abscissa -  $d_H/k$   
 ordinate -  $f$

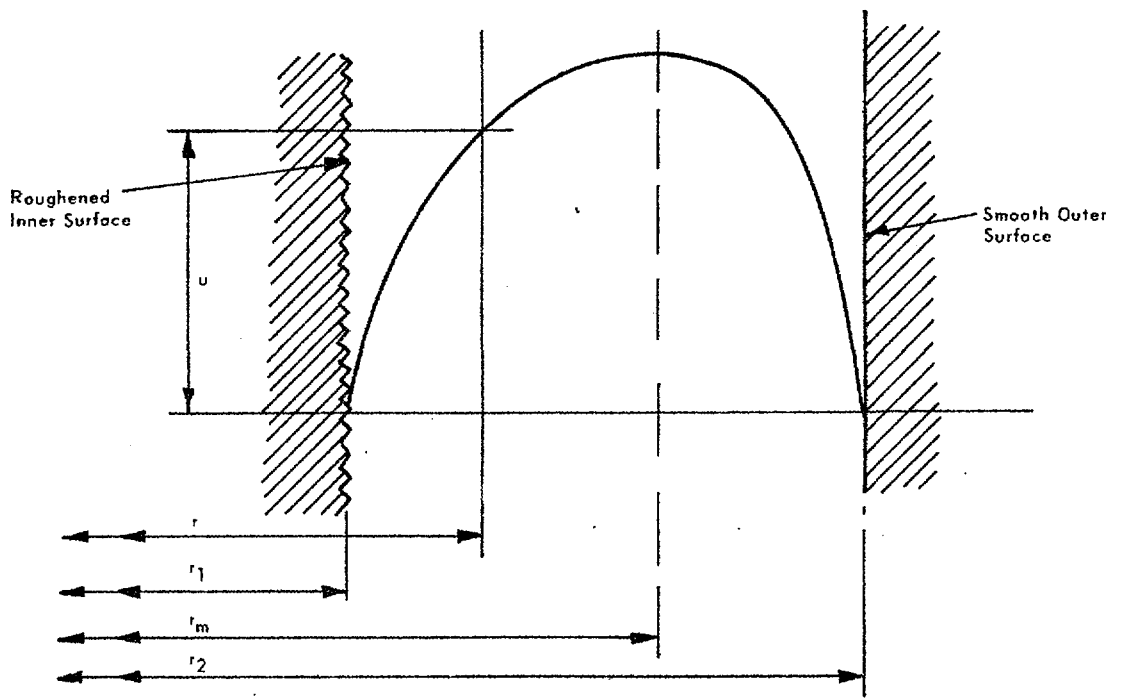


Fig. 45. Velocity distribution across annular passage ( $r_2 = r_o$ )

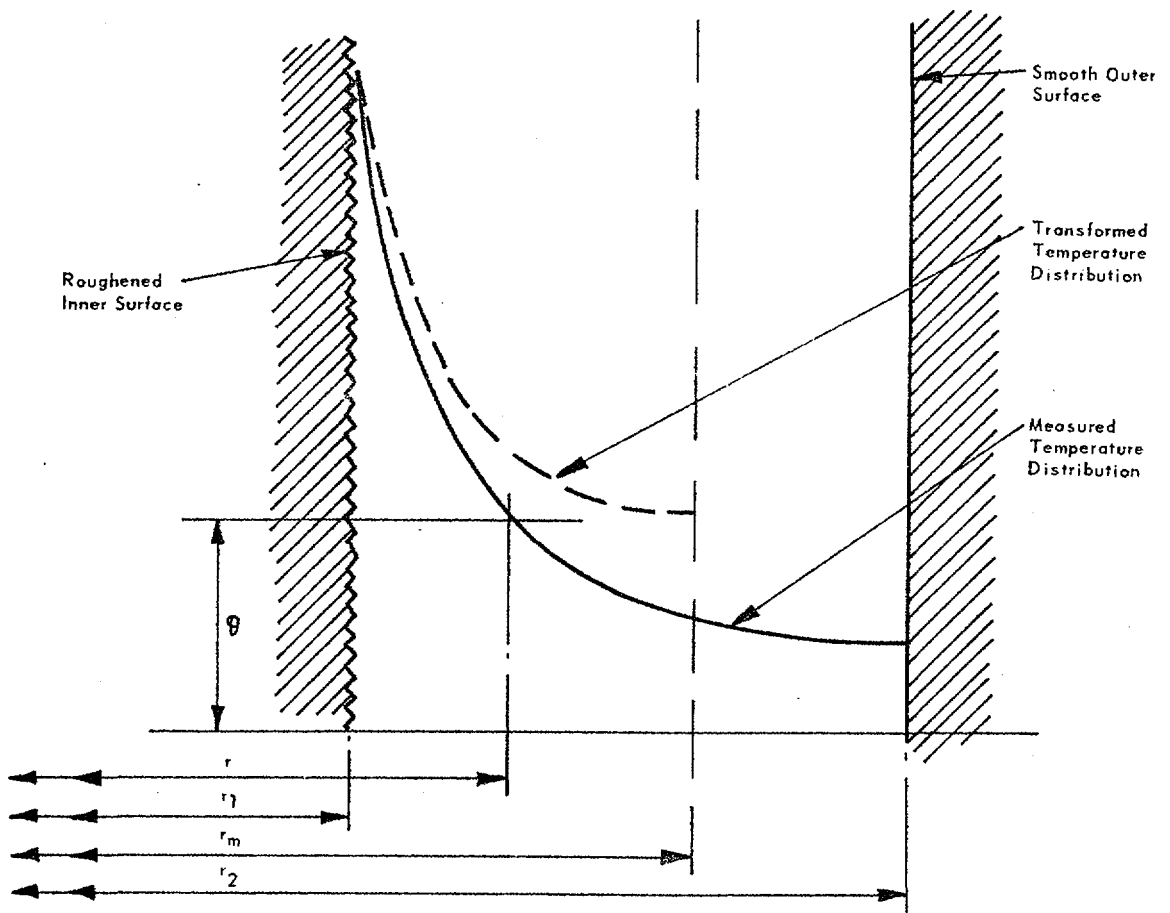


Fig. 46. Temperature distribution across annular passage ( $r_2 = r_o$ ).

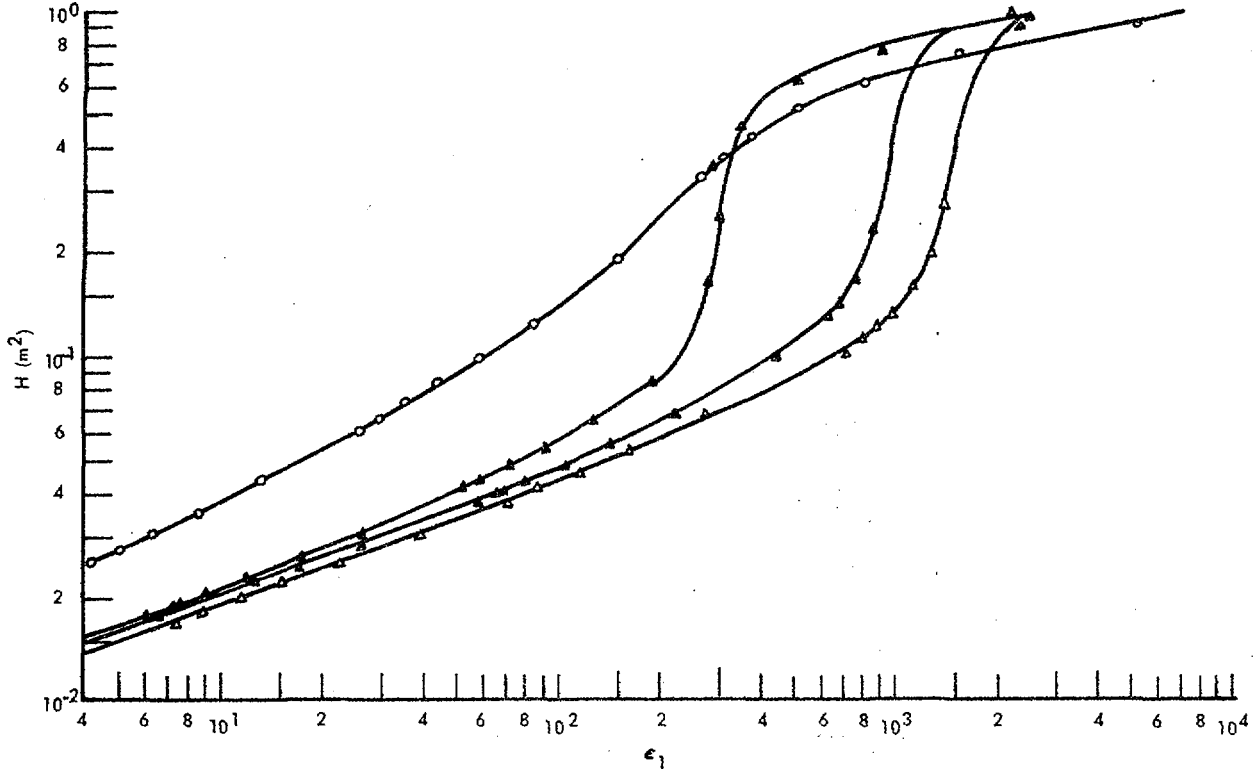


Fig. 47. Heating surface area  $H$ , dependent on performance figure for a narrow annulus. Inner tube has grooved indentations  $d_o/d_i = 1.287$ .

Distance  $p-b$  (mm) between grooves 0.0  $\Delta$ , 0.3  $\blacktriangle$ , 0.6  $\triangle$ :

Smooth inner tube 0

abscissa -  $\epsilon_1$

ordinate -  $H$  in  $m^2$

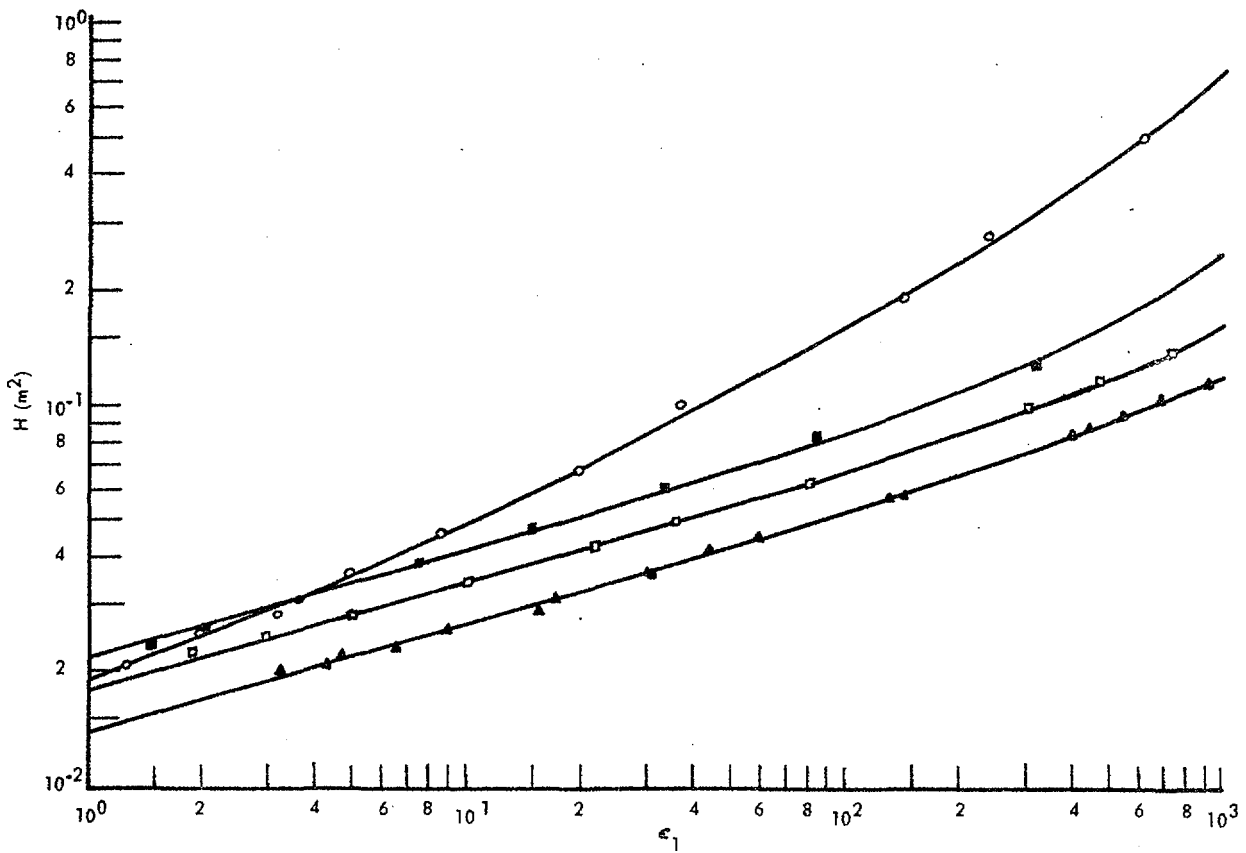


Fig. 48. Heating surface area  $H$ , dependent on performance figure for a wide annulus.

Inner tube ribbed  $d_o/d_i = 1.728$ ; Distance  $p-b$  (mm) ribs

2.5  $\blacktriangle$ , 5.0  $\blacktriangle$ , 10.0  $\square$ , 20.0  $\blacksquare$ ; Smooth inner tube 0.

abscissa -  $\epsilon_1$

ordinate -  $H$  in  $m^2$



LIST OF PUBLISHED AE-REPORTS

1-70. (See the back cover earlier reports.)

71. The space-, time- and energy-distribution of neutrons from a pulsed plane source. By A. Claesson. 1962. 16 p. Sw. cr. 6:—.
72. One-group perturbation theory applied to substitution measurements with void. By R. Persson. 1962. 21 p. Sw. cr. 6:—.
73. Conversion factors. By A. Amberntson and S-E. Larsson. 1962. 15 p. Sw. cr. 10:—.
74. Burnout conditions for flow of boiling water in vertical rod clusters. By Kurt M. Becker. 1962. 44 p. Sw. cr. 6:—.
75. Two-group current-equivalent parameters for control rod cells. Autocode programme CRCC. By O. Norinder and K. Nyman. 1962. 18 p. Sw. cr. 6:—.
76. On the electronic structure of MnB. By N. Lundquist. 1962. 16 p. Sw. cr. 6:—.
77. The resonance absorption of uranium metal and oxide. By E. Hellstrand and G. Lundgren. 1962. 17 p. Sw. cr. 6:—.
78. Half-life measurements of  $^6\text{He}$ ,  $^{16}\text{N}$ ,  $^{19}\text{O}$ ,  $^{20}\text{F}$ ,  $^{28}\text{Al}$ ,  $^{77}\text{Se}^m$  and  $^{110}\text{Ag}$ . By J. Konijn and S. Malmkog. 1962. 34 p. Sw. cr. 6:—.
79. Progress report for period ending December 1961. Department for Reactor Physics. 1962. 53 p. Sw. cr. 6:—.
80. Investigation of the 800 keV peak in the gamma spectrum of Swedish Laplanders. By I. O. Andersson, I. Nilsson and K. Eckerstig. 1962. 8 p. Sw. cr. 6:—.
81. The resonance integral of niobium. By E. Hellstrand and G. Lundgren. 1962. 14 p. Sw. cr. 6:—.
82. Some chemical group separations of radioactive trace elements. By K. Samsahl. 1962. 18 p. Sw. cr. 6:—.
83. Void measurement by the  $(\gamma, n)$  reactions. By S. Z. Rouhani. 1962. 17 p. Sw. cr. 6:—.
84. Investigation of the pulse height distribution of boron trifluoride proportional counters. By I. O. Andersson and S. Malmkog. 1962. 16 p. Sw. cr. 6:—.
85. An experimental study of pressure gradients for flow of boiling water in vertical round ducts. (Part 3). By K. M. Becker, G. Hernborg and M. Bode. 1962. 29 p. Sw. cr. 6:—.
86. An experimental study of pressure gradients for flow of boiling water in vertical round ducts. (Part 4). By K. M. Becker, G. Hernborg and M. Bode. 1962. 19 p. Sw. cr. 6:—.
87. Measurements of burnout conditions for flow of boiling water in vertical round ducts. By K. M. Becker. 1962. 38 p. Sw. cr. 6:—.
88. Cross sections for neutron inelastic scattering and  $(n, 2n)$  processes. By M. Leimdörfer, E. Bock and L. Arkeryd. 1962. 225 p. Sw. cr. 10:—.
89. On the solution of the neutron transport equation. By S. Depken. 1962. 43 p. Sw. cr. 6:—.
90. Swedish studies on irradiation effects in structural materials. By M. Grounes and H. P. Myers. 1962. 11 p. Sw. cr. 6:—.
91. The energy variation of the sensitivity of a polyethylene moderated  $\text{BF}_3$  proportional counter. By R. Fräki, M. Leimdörfer and S. Malmkog. 1962. 12. Sw. cr. 6:—.
92. The backscattering of gamma radiation from plane concrete walls. By M. Leimdörfer. 1962. 20 p. Sw. cr. 6:—.
93. The backscattering of gamma radiation from spherical concrete walls. By M. Leimdörfer. 1962. 16 p. Sw. cr. 6:—.
94. Multiple scattering of gamma radiation in a spherical concrete wall room. By M. Leimdörfer. 1962. 18 p. Sw. cr. 6:—.
95. The paramagnetism of Mn dissolved in  $\alpha$  and  $\beta$  brasses. By H. P. Myers and R. Westin. 1962. 13 p. Sw. cr. 6:—.
96. Isomorphic substitutions of calcium by strontium in calcium hydroxy-apatite. By H. Christensen. 1962. 9 p. Sw. cr. 6:—.
97. A fast time-to-pulse height converter. By O. Aspelund. 1962. 21 p. Sw. cr. 6:—.
98. Neutron streaming in  $\text{D}_2\text{O}$  pipes. By J. Braun and K. Randén. 1962. 41 p. Sw. cr. 6:—.
99. The effective resonance integral of thorium oxide rods. By J. Weitman. 1962. 41 p. Sw. cr. 6:—.
100. Measurements of burnout conditions for flow of boiling water in vertical annuli. By K. M. Becker and G. Hernborg. 1962. 41 p. Sw. cr. 6:—.
101. Solid angle computations for a circular radiator and a circular detector. By J. Konijn and B. Tollander. 1963. 6 p. Sw. cr. 8:—.
102. A selective neutron detector in the keV region utilizing the  $^{19}\text{F}(n, \gamma)^{20}\text{F}$  reaction. By J. Konijn. 1963. 21 p. Sw. cr. 8:—.
103. Anion-exchange studies of radioactive trace elements in sulphuric acid solutions. By K. Samsahl. 1963. 12 p. Sw. cr. 8:—.
104. Problems in pressure vessel design and manufacture. By O. Hellström and R. Nilson. 1963. 44 p. Sw. cr. 8:—.
105. Flame photometric determination of lithium contents down to  $10^{-3}$  ppm in water samples. By G. Jönsson. 1963. 9 p. Sw. cr. 8:—.
106. Measurements of void fractions for flow of boiling heavy water in a vertical round duct. By S. Z. Rouhani and K. M. Becker. 1963. 2nd rev. ed. 32 p. Sw. cr. 8:—.
107. Measurements of convective heat transfer from a horizontal cylinder rotating in a pool of water. K. M. Becker. 1963. 20 p. Sw. cr. 8:—.
108. Two-group analysis of xenon stability in slab geometry by modal expansion. O. Norinder. 1963. 50 p. Sw. cr. 8:—.
109. The properties of  $\text{CaSO}_4\text{Mn}$  thermoluminescence dosimeters. B. Bjärngård. 1963. 27 p. Sw. cr. 8:—.
110. Semianalytical and seminumerical calculations of optimum material distributions. By C. I. G. Andersson. 1963. 26 p. Sw. cr. 8:—.
111. The paramagnetism of small amounts of Mn dissolved in Cu-Al and Cu-Ge alloys. By H. P. Myers and R. Westin. 1963. 7 p. Sw. cr. 8:—.
112. Determination of the absolute disintegration rate of  $\text{Cs}^{137}$ -sources by the tracer method. S. Hellström and D. Brune. 1963. 17 p. Sw. cr. 8:—.
113. An analysis of burnout conditions for flow of boiling water in vertical round ducts. By K. M. Becker and P. Persson. 1963. 28 p. Sw. cr. 8:—.
114. Measurements of burnout conditions for flow of boiling water in vertical round ducts (Part 2). By K. M. Becker, et al. 1963. 29 p. Sw. cr. 8:—.
115. Cross section measurements of the  $^{58}\text{Ni}(n, p)^{58}\text{Co}$  and  $^{29}\text{Si}(n, \alpha)^{26}\text{Mg}$  reactions in the energy range 2.2 to 3.8 MeV. By J. Konijn and A. Lauber. 1963. 30 p. Sw. cr. 8:—.
116. Calculations of total and differential solid angles for a proton recoil solid state detector. By J. Konijn, A. Lauber and B. Tollander. 1963. 31 p. Sw. cr. 8:—.
117. Neutron cross sections for aluminium. By L. Forsberg. 1963. 32 p. Sw. cr. 8:—.
118. Measurements of small exposures of gamma radiation with  $\text{CaSO}_4\text{Mn}$  radiothermoluminescence. By B. Bjärngård. 1963. 18 p. Sw. cr. 8:—.
119. Measurement of gamma radioactivity in a group of control subjects from the Stockholm area during 1959-1963. By I. O. Andersson, I. Nilsson and Eckerstig. 1963. 19 p. Sw. cr. 8:—.
120. The thermox process. By O. Tjälldin. 1963. 38 p. Sw. cr. 8:—.
121. The transistor as low level switch. By A. Lydén. 1963. 47 p. Sw. cr. 8:—.
122. The planning of a small pilot plant for development work on aqueous reprocessing of nuclear fuels. By T. U. Sjöborg, E. Haefner and Hultgren. 1963. 20 p. Sw. cr. 8:—.
123. The neutron spectrum in a uranium tube. By E. Johansson, E. Jonsson, M. Lindberg and J. Mednis. 1963. 36 p. Sw. cr. 8:—.
124. Simultaneous determination of 30 trace elements in cancerous and non-cancerous human tissue samples with gamma-ray spectrometry. K. Samsahl, D. Brune and P. O. Wester. 1963. 23 p. Sw. cr. 8:—.
125. Measurement of the slowing-down and thermalization time of neutrons in water. By E. Möller and N. G. Sjöstrand. 1963. 42 p. Sw. cr. 8:—.
126. Report on the personnel dosimetry at AB Atomenergi during 1962. By K.-A. Edvardsson and S. Hagsgård. 1963. 12 p. Sw. cr. 8:—.
127. A gas target with a tritium gas handling system. By B. Holmqvist and T. Wiedling. 1963. 12 p. Sw. cr. 8:—.
128. Optimization in activation analysis by means of epithermal neutrons. Determination of molybdenum in steel. By D. Brune and K. Jirlow. 1963. 11 p. Sw. cr. 8:—.
129. The  $P_1$ -approximation for the distribution of neutrons from a pulsed source in hydrogen. By A. Claesson. 1963. 18 p. Sw. cr. 8:—.
130. Dislocation arrangements in deformed and neutron irradiated zirconium and zircaloy-2. By R. B. Roy. 1963. 18 p. Sw. cr. 8:—.
131. Measurements of hydrodynamic instabilities, flow oscillations and burnout in a natural circulation loop. By K. M. Becker, R. P. Mathisen, O. Eklind and B. Norman. 1964. 21 p. Sw. cr. 8:—.
132. A neutron rem counter. By I. O. Andersson and J. Braun. 1964. 14 p. Sw. cr. 8:—.
133. Studies of water by scattering of slow neutrons. By K. Sköld, E. Pilcher and K. E. Larsson. 1964. 17 p. Sw. cr. 8:—.
134. The amounts of As, Au, Br, Cu, Fe, Mo, Se, and Zn in normal and uraemic human whole blood. A comparison by means of neutron activation analysis. By D. Brune, K. Samsahl and P. O. Wester. 1964. 10 p. Sw. cr. 8:—.
135. A Monte Carlo method for the analysis of gamma radiation transport from distributed sources in laminated shields. By M. Leimdörfer. 1964. 28 p. Sw. cr. 8:—.
136. Ejection of uranium atoms from  $\text{UO}_2$  by fission fragments. By G. Nilsson. 1964. 38 p. Sw. cr. 8:—.
137. Personnel neutron monitoring at AB Atomenergi. By S. Hagsgård and C.-O. Widell. 1964. 11 p. Sw. cr. 8:—.
138. Radiation induced precipitation in iron. By B. Solly. 1964. 8 p. Sw. cr. 8:—.
139. Angular distributions of neutrons from  $(p, n)$ -reactions in some mirror nuclei. By L. G. Strömberg, T. Wiedling and B. Holmqvist. 1964. 28 p. Sw. cr. 8:—.
140. An extended Greuling-Goertzel approximation with a  $P_n$ -approximation in the angular dependence. By R. Håkansson. 1964. 21 p. Sw. cr. 8:—.
141. Heat transfer and pressure drop with rough surfaces, a literature survey. By A. Bhattacharyya. 1964. Sw. cr. 8:—.

Förteckning över publicerade AES-rapporter

1. Analys medelst gamma-spektrometri. Av D. Brune. 1961. 10 s. Kr 6:—.
2. Bestrålningsförändringar och neutronatmosfär i reaktortrycktankar — några synpunkter. Av M. Grounes. 1962. 33 s. Kr 6:—.
3. Studium av sträckgränsen i mjukt stål. G. Ösberg, R. Atterma. 1963. 17 s. Kr 6:—.
4. Teknisk upphandling inom reaktorområdet. Erik Jonson. 1963. 64 s. Kr. 8:—.

Additional copies available at the library of AB Atomenergi, Studsvik, Nyköping, Sweden. Transparent microcards of the reports are obtainable through the International Documentation Center, Tumba, Sweden.